EUROPEAN AVIATION SAFETY AGENCY
AGENCE EUROPÉENNE DE LA SÉCURITÉ AÉRIENNE
EUROPÄISCHE AGENTUR FÜR FLUGSICHERHEIT

Research Project EASA.2009/3

LIBCOS - Load upon Impact Behaviour of Composite Structure

easa.europa.eu

Disclaimer

This study has been carried out for the European Aviation Safety Agency by an external organization and expresses the opinion of the organization undertaking the study. It is provided for information purposes only and the views expressed in the study have not been adopted, endorsed or in any way approved by the European Aviation Safety Agency. Consequently it should not be relied upon as a statement, as any form of warranty, representation, undertaking, contractual, or other commitment binding in law upon the European Aviation Safety Agency.

EASA.2009.OP.24
LIBCOS – Significance of Load upon Impact Behaviour of Composite Structure

Final report

Nathalie Toso & Alastair Johnson

German Aerospace Center (DLR)
Institute of Structures and Design
Pfaffenwaldring 38-40
70569 Stuttgart

8 November 2011

Contents

Executive Summary

A critical safety issue for the design of primary aircraft structures is vulnerability and damage tolerance due to foreign object impact from bird strike, hail, tyre rubber and metal fragments. The damage tolerance strategy for the aircraft industry is based on defining critical damage states for composites which are linked to damage visibility and hence damage detection during service. Currently impact tests on aircraft structures are carried out on test specimens supported in a test fixture in a stress-free condition. However aircraft fuselage and wing structures in flight are subjected to quasi-static loads up to design limit load, hence foreign object impacts usually occur on preloaded structures which may influence damage tolerance. This study focuses on a comprehensive test programme investigating the influence of pre-loads on the residual strength of composite generic panels after impact, representative of fuselage bay panels. To that aim, a total of 78 tests have been conducted: 57 on composite plates and 21 on aluminium plates for comparison.

The test programme used representative composite fuselage bay panels situated between frames and stringers. Material selected is an aerospace UD carbon epoxy prepreg Cycom 977-2-35-12KHTS-134-300 from Cytec. Plates with impact area 500 mm x 170 mm are loaded in axial tension or compression in a new hydraulic pre-stressing frame designed to fit in the DLR gas gun target chamber. Pre-load level in tension is chosen equal to 0.25% strain, which is representative of design limit loads (DLL) for fuselage panels. In compression the considered preload levels are 0.5 Pb (unbuckled state) and 1.4 Pb (post-buckle state) for the composite plates, and 1.5 Pb for the aluminium plates where Pb is the compression buckling load of an undamaged plate. The reason for conducting investigation in the postbuckle region is that buckling may occur in these thin panels at DLL. For preloading in the postbuckle region, two cases are investigated corresponding to an impact on the concave and convex face of the buckle. Impact tests are carried out with a 60 mm diameter gas gun at velocities in the range 64 – 136 m/s, and impact energies 36 – 125 J. Two main impact scenarios were considered: notch damage from a 12 mm steel cube projectile, representative of impact from engine fragments or metal objects; blunt impact damage from glass balls (Ø24-25 mm), which could represent hail or runway stone debris. Impact damage is detected by visual inspection and quantified with lock-in thermography, especially for delamination. Depending on the preload regime, corresponding residual strength tests were carried out on each plate.

The following main conclusions can be drawn from the experimental results:

- For the aluminium plates there is no significant interaction between tension/compression preload and impact damage, at the DLL preload levels considered, which would cause reduction in residual strengths.
- For the composite plates in tension there are small reductions in residual strengths for both blunt and notch impacts. They are not very significant for the low preloads at DLL level studied here.
- For the composite plates in compression with notch damage, which were all tested and failed by buckling, there is no significant reduction in residual compression strengths. At buckling failure, due to the preferred buckling mode, the high failure strains are away from the central damaged area with penetration holes, which may explain the small influence of pre-loading on the residual strength. If the buckling modes were different, which will be the case for different plate geometries, results may then be different.
- The composite plates in compression with blunt impact causing delamination damage are the most critical cases studied. Delaminations grow with quasi-static loads which have a strong influence on ultimate bending strengths and hence reduce buckling failure loads.

This first study shows that compression pre-load and blunt impact may be a critical case for the damage tolerance of composite panels. This was observed in the DLR study for a specific plate configuration (lay-up, dimensions), and specific preload cases 0.5 Pb (prebuckling) to 1.4 Pb (post-buckling), with blunt impacts at energy levels 58.4 – 74.0 J.

Acknowledgements

This work was funded by European Aviation Safety Agency (EASA). The authors wish to thank Simon Waite for his guidance and constructive criticism throughout the project, Werner Kleine-Beek for project management and Emmanuel Isambert for project coordination.

This study would not have been possible without the active participation of the DLR test team: Albert Reiter (gas gun testing), Harald Kraft (quasi-static testing, instrumentation), Husam Abu El-Hija (quasi-static testing) and Rodolfo Aoki (non-destructive testing).

Glossary

ACJ	Advisory Circular Joint
ADL	Allowable Damage Limit
AIA	Aerospace Industries Association
ALCAS	Advanced Low Cost Aircraft Structures
AMC	Acceptable Means of Compliance
BVID	Barely Visible Impact Damage
CAI	Compression After Impact
CDT	Critical Damage Threshold
CELPACT	Cellular Structures for Impact Performance
CFRP	Carbon Fibre Reinforced Plastics
CMH	Composite Materials Handbook
CS	Certification Specifications
CT	Computer Tomography
DLL	Design Limit Load
DLR	Deutsches Zentrum für Luft- und Raumfahrt (German Aerospace Center)
DT	Damage Tolerance
DUL	Design Ultimate Load
EASA	European Aviation Safety Agency
E_D	Impactor kinetic energy at onset of delamination
E_F	Impactor kinetic energy at onset of fracture
FAR	Federal Aviation Regulations (Title 14 of US Code of Federal Regulations)
FOD	Foreign Object Damage
HVI	High Velocity Impact
LAP	Laminate Analysis Program
LIBCOS	Significance of Load upon Impact Behaviour of COmposite Structure
LL	Limit Load
LVI	Low Velocity Impact
LWIR	Long-Wavelength InfraRed
MCT	Mercury Cadmium Telluride
MoC	Means of Compliance
NDA	Non-disclosure Agreement
NDE/NDT	Non Destructive Evaluation / Non Destructive Testing
NPA	Notice of Proposed Amendment
Pb	Plate buckling load
P_F	Plate ultimate failure load
Q/S	Quasi-Static
RSF	Residual Strength Factor
UD	Unidirectional
UL	Ultimate Load
VID	Visible Impact Damage

1 Introduction

The route to certification adopted by the aircraft manufacturers is based on the well known test pyramid for aircraft structures, Fig. 1, which typically foresees 5 levels of tests from materials test coupons in level 1 up to full aircraft structures in level 5. As described by Hachenberg [1], the certification of primary aircraft structures is governed by the airworthiness requirements FAR-25 [2], EASA CS-25 [3] for large transport aircraft. For composite materials the means of compliance recommendations ACJ 25.603 [4] (now replaced by AMC 20-29 [5]) and FAA AC 20.107A [6] of the airworthiness authorities are applied. Besides material and manufacturing qualification the main requirement is proof of strength as follows:

- proof of static strength
- proof of residual strength after fatigue cycling
- proof of damage tolerance

From the structure mechanical view additional proofs are required for:

- crashworthiness and ditching
- explosion protection
- severe impact and discrete-source damage: turbine blade failure, bird impact, hail impact, tyre fragment impact, etc.

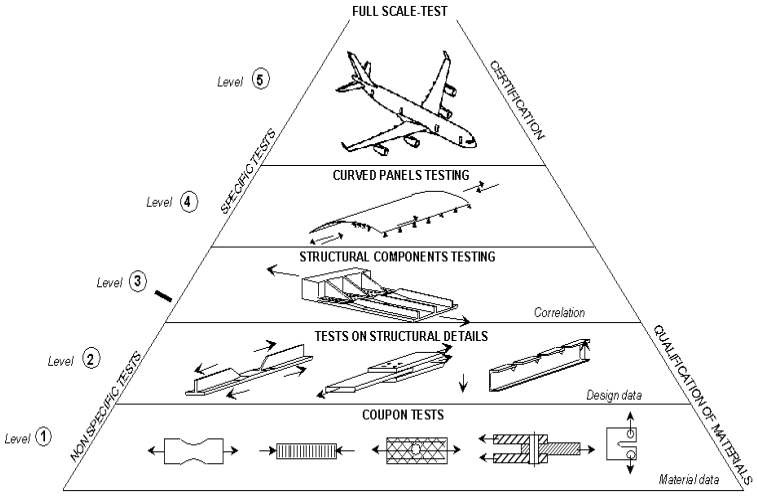

Fig. 1: Suggested pyramid of physical tests used to support aircraft design and certification [1]

Compliance to the requirements may be demonstrated either by means of testing or analysis. While the proof of static strength is produced both experimentally and analytically, proof of fatigue and damage tolerance is generally produced experimentally. When considering aircraft vulnerability issues such as fuselage crash response and high velocity impact (HVI) from birds, hail, runway debris, burst tyre fragments it is apparent from Fig. 1 that tests are required at each level of the pyramid. Level 1 tests are to determine materials properties for design analysis, with levels 2 and 3 representing structural elements of increasing complexity, such as dynamically loaded joints, crash absorbers, frame stiffened panels, etc. At level 4 a test programme might consist of HVI gas gun tests with larger stiffened panels impacted by tyre rubber fragments, hail or metal fragments. Finally at the level 5 full scale structure it will be necessary to carry out bird strike tests on wings and front cockpit.

The damage tolerance strategy is based on defining critical damage states for composites which are linked to damage visibility and hence damage detection during service. For composite materials this is currently being developed in the CMH-17 guidelines [7] as a MoC

for damage tolerance. A key element here is the definition of damage Categories 1 – 5. Category 1 (barely visible impact damage, BVID) is based on a *no-growth* concept, meaning that damages up to the boundary of optical detectability, will not grow under operational loads and will not cause a loss of the residual strength below design ultimate load level (*DUL*). Category 2 and 3 are visible impact damage (VID) seen in routine and visual inspections. Here the residual strength may not fall below design limit load level (*DLL*) corresponding to maximum operational load cases. Category 4 is high energy discrete source damage which is obvious to the pilot such as rotor burst and some bird strikes, lightning strikes and tyre debris threats. Here the aircraft has a 'get you home' requirement with limited flight manoeuvres at below DLL through redundancy in the initial aircraft design and secondary load paths. Category 5 damage is more severe discrete source damage due to rare events, which grounds the aircraft.

With the advent of new materials such as composites specific guidelines are issued [4], [6] and requirements such as [2], [3] are continually revised as more experience with the materials becomes available. It may be that existing design and certification strategies are unsuitable or inadequate for composite structures. Before new guidelines are developed it is necessary to have a clear knowledge of relevant materials and structural behaviour, particularly when the failure behaviour of composites is different to that of metals which is the case under HVI loads. This is thought to be the case when statically loaded structures are subjected to additional impact loads, which is the motivation for the LIBCOS project. It is proposed in LIBCOS to carry out a detailed study of high velocity impact behaviour on loaded composite specimens and structural elements at Levels 1 and 2 of the test pyramid, in order to develop an understanding of basic phenomena. Following the discussion of damage tolerance requirements above, it is proposed that the critical load cases for experimental study are panel structures subjected to Category 3 and 4 discrete source impact damage, in combination with static preloads up to DLL arising from flight loads or fuselage pressures. The results on both composite and metallic panels will be analysed with the current damage tolerance MoC to decide if new or modified guidelines are needed for this combined load case. Recommendations will be made to EASA for amending certification requirements and MoC, together with a methodology for future studies at higher levels of the test pyramid which would be required to validate any new guidelines introduced.

There have been a number of experimental studies on influence of preload on impact response of composite plates and structural elements, [8] - [12]. Study of this recent literature shows interaction effects between preload and impact damage, but the work is not systematic enough to provide clear guidelines for improving or changing aviation safety requirements. Some are only relevant to BVID damage, whilst the study in [12] with high energy impacts from low velocity drop tests is not strictly relevant to Category 4 discrete source impact from bird strike, metal fragments etc. This gives a strong motivation in the present study to propose a series of composite flat plate tests, with typical specimen size 500 x 200 mm representing an idealised fuselage bay or wing panel, which is preloaded in both tension and compression at strain levels typical of aircraft DLL. Then to carry out systematically gas gun impact tests with predominantly hard debris and softer bodies to produce typical notch damage or delamination damage. Steel cubes and steel beams are appropriate as typical hard debris projectiles for notch damage. Delamination damage may be achieved with tyre rubber fragments, which are quicker to prepare than ice or gelatine synthetic bird tests. Delamination damage is also observed in blunt impact with stone and concrete projectiles, which may be simulated experimentally by glass balls.

The discussion above of damage tolerance certification requirements for composite aircraft structures leads to the definition of the main objectives in the current project. These are:

1. Carry out a systematic experimental test programme of gas gun impact tests with selected projectiles which cause both notch and delamination damage on representative aircraft carbon composite panels under both tension and compression preloads.

2. Repeat the impact test series with preloads on aluminium test panels under equivalent design load conditions.
3. Apply NDE inspection methods (both before and after test) to all tested panels to define and establish damage levels and their visible detectability.
4. Measure residual tensile or compression strengths of the test panels, depending on preload condition, and analyse influence of preload and impact conditions on residual strengths.
5. Assess the influence of preload on composite and metallic panels in the context of aircraft safety and damage tolerance requirements. If appropriate make recommendations for changes to existing certification requirements or special conditions, and propose acceptable means of compliance.

2 Test equipment and specifications

For this study, DLR will use the following facilities:

- Gas gun impact test facilities
- Pre-stressing fixture
- Quasi-static structural testing machine
- NDE - lock-in thermography and eventually Computer tomography

2.1 DLR gas guns and equipments

In the DLR HVI test facility, which is operational since January 2006, three gas gun calibres are available: 200 mm, 60 mm and 32/25 mm. The 60 mm gas gun was used in LIBCOS as it was compatible with the selected panel widths of 200 mm and projectile sizes, up to 30 mm wide. It consists of a single 50 l pressure tank and a fast acting pneumatic valve to a dove-tail breech and 5m long honed bore barrel. The projectile masses here are in the range of 0.01 - 0.5 kg with impact speeds up to 200 m/s, depending if air or helium is used as pressurized medium. The automatic system is designed for a maximum working pressure of 8 bars.

The muzzles of the 60 mm guns are fully enclosed in a 4m long by 2.7m wide by 2.4m high steel target chamber fitted with sliding doors and four large polycarbonate windows for viewing and filming. Fig. 1a shows the target chamber set up after a tyre rubber test with the 200 mm gun on a composite shell structure attached to the support frame. The 60 mm gun muzzle is at the bottom right of the photograph. Fig. 1b shows a typical set up for plate impact in LIBCOS with the 60 mm gun and the preload fixture.

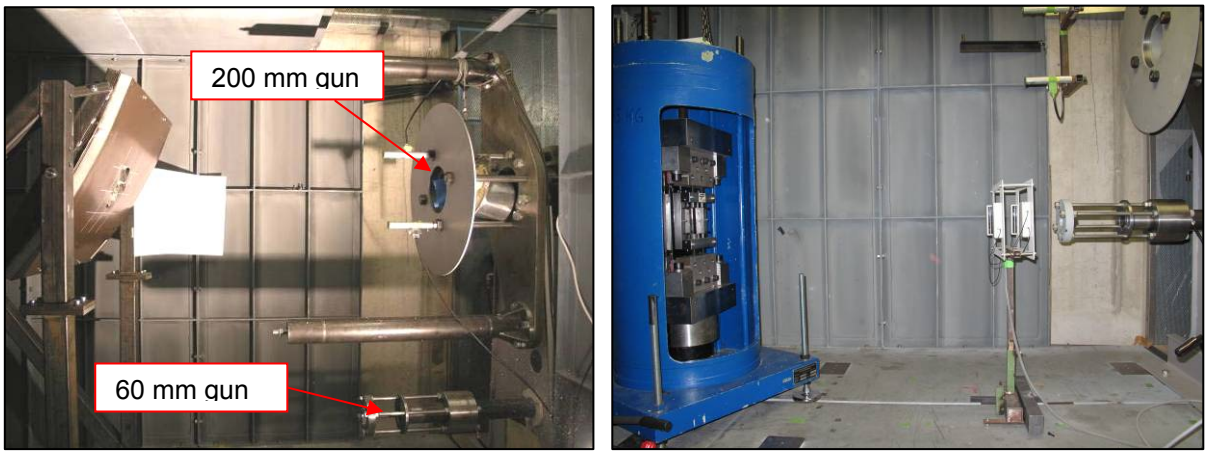

a) b)

Figure 1: DLR Target chamber for 200 mm and 60 gas guns
a) Tyre rubber impact on 800 mm x 800 mm curved sandwich shell with 200 mm gun
b) 60 mm gun with preload test fixture

In the 60 mm gun, the projectiles are held in sacrificial polyurethane foam cylinders inserted in aluminium alloy ‘cups’. These ‘*sabot*’ devices hold the projectile in the desired orientation and form a gas tight seal against the driving gas. A cavity at the front of the sabot whose diameter and depth are adapted to the size and geometry of the projectile carries the projectile. A sabot stripper is fitted onto the muzzle of the barrel which restricts the muzzle opening such that the projectile can pass through unimpeded whilst the sabot is stopped. The velocity of the projectile is measured by an optical gate with three IR sensor pairs sited 50mm apart. The velocity meters are positioned directly behind the muzzle and are linked to

a PC for computing the velocity and synchronising the start of cameras and other measuring devices, if being used.

During the HVI-tests the free flight and the impact of the projectiles on the target structure may be visualised through a high-speed camera or a high-speed video camera. The HVI facility is equipped with a PC controlled high speed digital camera system (PHOTRON Fastcam Ultima APX RS, Model 250k) comprising a 10 Bit CMOS monochrome sensor with 1024x1024 pixel. Large pixel size provides high light sensitivity. The camera speed is 60 - 3000 full frames per second (1024x1024 pixel) up to 250 000 split frames per second (128x16 pixel). A frame frequency of 50 000 frames per second still provides a resolution of 128x144 pixel. The shutter speed goes up to 1 μs. The recording time is 1s with 2000 full frames per second with the standard storage depth and has an option of 3s with 200 f/s with extended storage. Of high importance is a variable pre-/post-trigger option. The camera is equipped with a high quality zoom lens system (24 - 85mm) and with control and download software. The system provides data formats such as JPEG, AVI, TIF, and BMP. Flash light is the most appropriate light source for the system to generate good quality film, however all standard high speed film light sources (“cold light”) work well.

Dynamic test data may be obtained by strain gauges attached to the test structure and for specimens mounted directly onto load cells, load pulse data may be determined. All data from strain gauge signals and the velocity meter outputs are recorded in a multi channel transient recorder. The recorder comprises two units – one unit with 10 channels having a sample rate of 1/10 μs with a 8 bit resolution and a second unit with 24 channels and a sample rate of 1 μs with a 12 bit resolution. The units have trigger options of 1 - 100% delay (pre-/post-trigger). The data volume of all channels is 1MB.

DLR has experience with the firing of several types of metallic projectiles:

- Steel ball with a diameter of 15 mm and mass 13.6 g,
- Steel cube with a side length of 12 mm and mass of about 13 g,
- Steel beam with the dimensions 30 mm x 4 mm x 108 mm and mass 100 g.

Figure 2 shows a steel beam projectile with and without the ‘sabot’. HVI tests with these projectiles enable to test the impact of metallic objects on the fuselage/wing, typical scenarios being:

- Runway debris projected by the tyres or from the blast of the engines against the fuselage
- Engine debris flying out of the aero-engines or propellers

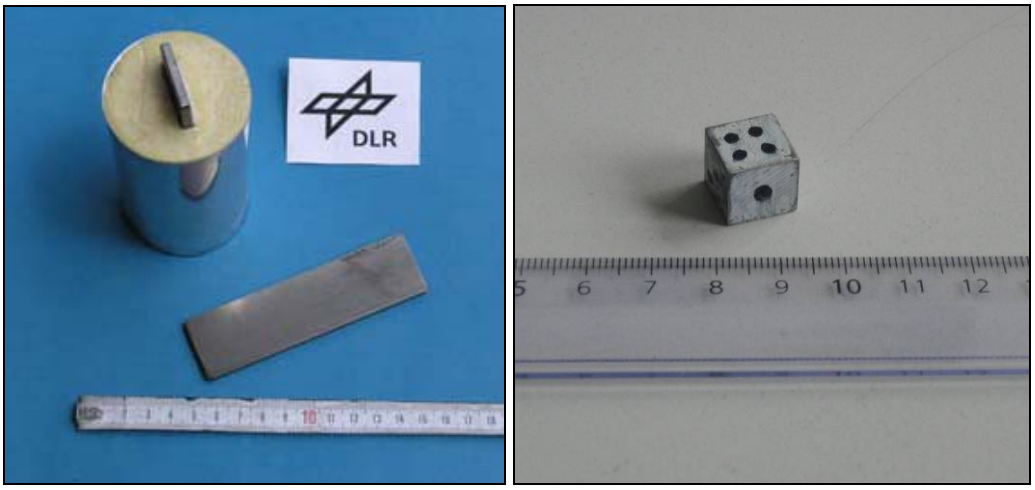

Figure 2: steel beam and its sabot / 13 g steel cube

The rubber projectiles as seen in Fig. 3 were cut from aircraft tyres provided to the DLR by Airbus and EADS in earlier studies. In order to have a straight rubber beam with an acceptable weight around 100 g, it was necessary to build the rubber projectiles by using two strips cut from the tyre, consisting of tyre rubber and fabric reinforcements. These two strips were attached to each other by using special adhesive adapted to rubber. The dimensions of the rubber projectiles are 30 mm x 24 mm x 134 mm where each strip is 30 mm x 12 mm x 134 mm.

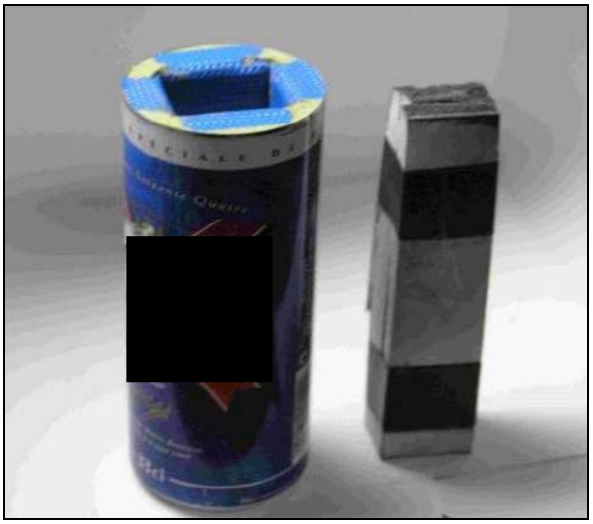

Figure 3: rubber beam and its sabot

Due to similar density to stones or concrete debris and for the reproducibility, glass balls (Fig. 4) are used as substitutes for the impact of stones on a structure. Within the LIBCOS test campaign, several glass balls were used to cause delamination damage to the test plates:

- Ø24 mm , 18 g
- Ø24.5 mm , 19.3 g
- Ø25 mm , 20.2 g

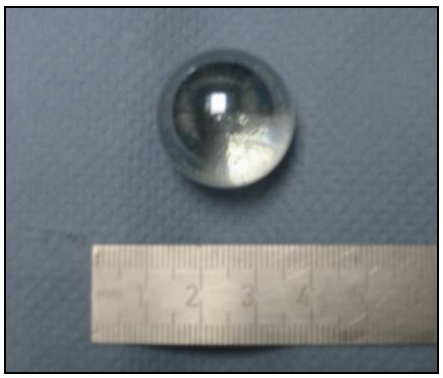

Figure 4: glass ball as substitute for stone impact

According to the regulatory threats, following impactors and associated speeds are reported.

- In the case of engine uncontained rotor event, the fragments are generally described as large, intermediate and small (shrapnel) according to [13]. For each of the fragment classes, typical sizes are 20”, 5” and 1-1.5” respectively. They are typically modelled in the A/C by 1/3 disk for large fragment, 1/3 bladed radius or 1/30 of the bladed disk mass for intermediate fragment and the outer half of a blade airfoil or outer 1/3 airfoil in the case of a fan blade for small fragments. Impact energies to consider are not defined more specifically than the translational energy (neglecting

rotational energy) of the fragment travelling at the speed of its c.g. location [14]. Historical data [15] from uncontained engine failure reports velocities between 97.5 m/s and 514.5 m/s and masses between 45 g and 4.62 kg. As stated in §25.963(e) [3], the following may be used for evaluating access covers (located within 15 degrees forward of the front engine compressor or fan plane) for impact resistance engine debris in the absence of relevant data: “an energy level corresponding to the impact of a 9·5 mm (3/8 inch) cube steel debris at 213.4 m/s (700 fps), 90 degrees to the impacted surface or area should be used”.

- In the case of tyre impacts, the segments to be considered should represent 1% of the tyre mass and the impact area is distributed over an impact area equal to 1.5 % of the total tread area. The velocities used in the assessment should be based on the highest speed that the aircraft is likely to use on the ground under normal operation.[14]
- Runway debris are usually simulated with standardised hemispherical steel impactors with tip diameters 0.5-1 inch (13-25 mm). Impact energies are limited when attempting to create BVID damage levels associated with tool drops and runways debris. They typically range from 20 to 140 J [16].
- Ground hail diameters typically range from 0.4 to 1 inch (10-25 mm) while impact energy cutoffs range between 2 and 56 J. Small in-flight hail with the same size is also addressed in category 1 damage with velocities up to the cruise velocity of the aircraft. When considering severe in-flight hail (category 2 damage), hail diameters of approximately 2 inches (50 mm) are typically used with energies of up to 32 J for ground hail and velocities up to the vehicle’s cruise velocity for in-flight hail. [16]

As CFRP plates are very sensitive to the damage mode (notch and delamination), it was decided to conduct a preliminary impact test campaign with impactors likely to cause each of these damage modes. To that aim following impactors and impact velocities were investigated:

- 100g steel beams (dimensions 30 mm x 4 mm x 108 mm) with velocities in the range 65 – 75 m /s and 13 g steel cubes (12 mm side length) with velocities in the range 60-135 m/s for notch damage,
- 100g Rubber beams (dimensions 30 mm x 24 mm x 134 mm) at approximately 100 m/s and 18-20 g glass ball (24-25 mm diameter) with velocities in the range 60-85 m/s.

The glass balls were selected to provide a reproducible projectile for blunt impact delamination damage in composite plates. Referring to the regulatory threats they could represent runway debris, such as stones and concrete fragments, and from the mass and energy considered they will provide similar damage to hail on the ground. Steel balls are less suitable for these impact scenarios, since for the same mass they have much smaller diameters which DLR experience has shown may cause notch damage.
For the aluminium plate, the same projectiles are used with a range of velocities leading to either indentation or notch. Tests up to level 2 of the pyramid of physical tests (Fig. 1) are carried out in this study.

2.2 Pre-stressing fixture

At the DLR Institute of Structures and Design, a loading frame for the pre-stressing fixture was already available. It can accept plates with 250 mm x 750 mm dimensions. This frame was extended/upgraded according to the principles shown in Fig. 5 for applying pre-stressing under compression or tension. As it was decided to use a force driven pre-stressing, a hydraulic cylinder jack is used to apply the pre-stressing loads (max. 1000 kN). Depending on its location and mode of operation, compression or tension loads may be applied.

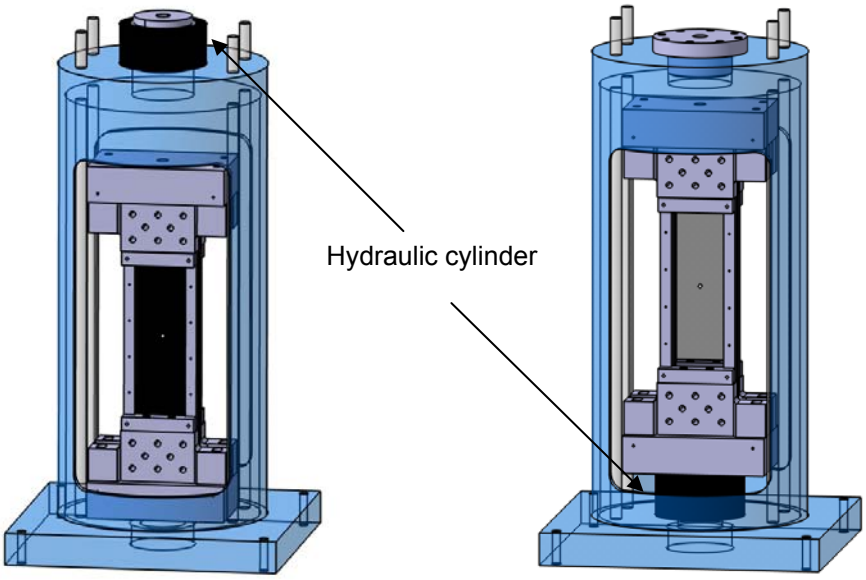

Figure 5: Design of the pre-stressing fixture

The test fixture is mounted on 4 adjustable feet, which enable the point of impact on the test plates to be specified. The configuration of the pre-stressing fixture is shown in Fig. 6 for both tension and compression preload tests. The test plates are clamped at the ends for correct load introduction. The long sides are supported by two pairs of rails built into the loading frame with knife edge contact at the plates. The long edges were supported 15 mm inside the plate boundaries, with the consequence that 200 mm wide test plates had an effective width for impact loading of 170 mm.

Figure 6: Pre-stressing fixture for tension (left) and compression (right) pre-loading

2.3 Quasi-static structural testing

For the standard quasi-static tests, DLR has available three servo-hydraulic universal-axial testing machines. These axial testing machines are suited for investigation of specimens with a small cross section under precise axial loading. The machine is driven by an internal waveform generator. For special testing tasks, a supplementary PC with a 16 bit A/D converter is used. This combination allows the application of any desired loading distribution. For the LIBCOS study, a Zwick 1494 machine was used (Fig. 7). Technical data are available in Table 1. Clamping jaws for specimens with a diameter of 100 mm are available and were used for the residual strength tests. In order to apply loads to the 200 mm wide plate specimens from these smaller grips, load was transferred through stiff 200 mm wide aluminium tabs bonded onto the composite and aluminium plates, as is seen in Fig. 9.

Table 1: Technical data of the Zwick 1494 (Fa. Zwick)

load	± 500 kN
max. traverse path	850 mm
max. testing velocity	200mm/min
temperature range	up to 180° C
max. workspace (B x H)	B = 630 mm; H = 1000 mm
clamping pressure	up to 480 bar
control	manually, path and power controlled

Figure 7: Zwick 1494 test machine (Fa Zwick)

2.4 Damage assessment

For post-test investigations of impact damage a number of NDE techniques are available at the DLR Institute of Structures and Design: ultrasonic C-Scan, lock-in thermography and X-ray based computer tomography (CT). Lock-in thermography as shown in Fig. 8 may be used for a non-contact evaluation of skin damage. The advantage of this technique over ultrasonic inspection is that it requires no contact, it is fast, and large structures can be inspected [17]. The main disadvantage is that the damage is not always clearly represented and skill is required in setting up the equipment and understanding the influence of frequency on the signals. Because of the large number of specimens in LIBCOS and the need for rapid NDE evaluation between HVI test and residual strength test, thermography was used for assessment of damage.

Figure 8: Lock-in thermography

Each plate was inspected using a CEDIP JADE III LWIR (7.7 ~ 9.3µm) infrared camera. The 320 x240 LWIR MCT focal plane detector array responds to radiation in the 3-5 µm spectral band at a frame rate up to 200 Hz. The camera is equipped with a Stirling cooling and the thermal sensitivity is 35mK. A lockin module and a signal generator control the light source (generating the thermal waves) which is synchronised to the recording process of thermal images. In the present task four modulated heating lamps were used. After several images (<1000) are recorded over several modulation cycles a Fourier analysis is performed at each pixel resulting in a local amplitude and phase modulation.

The thermal diffusion length is dependent on the thermal diffusivity of the material and the modulated frequency of the thermal waves:

$$\mu = (\alpha / (\pi f))^{1/2}$$

µ: thermal diffusion length;
α: thermal diffusivity; (4.10^{-3} cm²/s)
f: frequency

The phase angle between the sinusoidal illumination of the sample surface and the local thermal wave response (affected by reflection from defects) is colour coded and

visualized on the monitor as a phase angle image of the inspected surface area. Multiplying the inspection depth by 2 requires a reduction of frequency by 4. Common amplitude thermography pictures do not show depth information.

The evaluated lockin thermography images are phase angle images that reveal areas of hidden inhomogenities in the depth. In this report the images in Annex B are phase image pictures at 0.05 Hz showing the front and the rear views of the LIBCOS composite plate specimens.

3 Materials and test procedures

3.1 Materials selection

It is important in the LIBCOS project to use typical industry standard composite materials from civil transport aircraft and to select representative laminates and geometries of aircraft wing or fuselage panels. Furthermore the composite materials chosen should be readily available in the quantities required for the test programme. DLR has worked with Airbus in a number of EU and German national research projects on wing and fuselage structures, the most recent being [18] – [19]. In the CELPACT project Airbus proposed the UD carbon/epoxy prepreg Cycom 977-2-35-12KHTS-134-300 from Cytec as being suitable for the manufacture of composite fuselage panels and sandwich panel skins. As this prepreg is freely available from Cytec without an NDA it was decided to use this as the basis for LIBCOS and 3 rolls each with 75 m² were purchased by the DLR.

There is no standard laminate layup for an aircraft fuselage bay panel. As discussed in [20] the fuselage panels are placed into load categories which depend on design loads and position in the fuselage. Then layup is specified and optimised for each load category. A starting point could be a quasi-isotropic layup, with additional 0° plies for different levels of axial tension or compression load. Two generic laminate layups were selected, as indicated in Table 2. These are Lam. A a symmetric 17 ply lay-up with nominal thickness 2.125 mm for the tension loaded panels and Lam. B a 25 ply lay-up with thickness 3.125 mm for the compression loaded panels. The layup notation in the table indicates the % of plies in the (0°/±45°/90°) directions to the plate long axis. Note that a quasi-isotropic plate has layup (25/50/25), so that both panels here are reinforced by additional 0° plies.

Table 2: Generic aircraft fuselage panel layups

Lam.	Thickness	Lay-up	Application
A	2,125	17 UD plies (35/47/18) layup	Tensile preloads
B	3,125	25 UD plies (40/48/12) layup	Compression preloads

Aluminium 2024T3 was selected as typical aeronautical material for the manufacture of the aluminium specimen plates. A discussion point was how to select equivalent aluminium panels to the proposed composite panels. This is difficult since a bay panel in a composite aircraft structure will have different geometry and load conditions to an aluminium panel due to different design concepts and structure configuration. Preliminary calculations were carried out by the DLR to determine panel tensile failure loads and axial buckling loads for the composite and aluminium panels being considered, as summarised in Table 3. It was found that the tensile preload to achieve 0.25% axial strain for a 2 mm aluminium plate was 73 kN compared with 69.9 kN predicted in the chosen 2.125 mm composite plate. It was therefore decided to base the aluminium tests on 2 mm thick plates with the same geometry as the composite panels. It follows that ultimate tensile loads will be different between composite and aluminium plates, due to the higher laminate strength in the load direction, and buckling loads will also be different due to different flexural properties. Large aluminium 2024T3 panels, with thickness 2 mm, were purchased from ALMET GmbH near Stuttgart and cut by them into 750 x 200 mm plates for the LIBCOS tests.

3.2 Design and manufacture of plate specimens

For a transport aircraft composite fuselage a typical frame pitch is considered to be in the range 530 mm – 635 mm, with stringer spacing in the range 130 mm – 200 mm. Using this information, it was decided to base the LIBCOS test programme on a typical fuselage bay

panel situated between frames and stringers, and a basic plate geometry of 500 mm x 200 mm was selected as standard. For the gas gun impact tests lateral supports are required, which were 15 mm from the long edges of the plate. Thus the impacted size of the plates is 500 mm x 170 mm which is representative of a composite fuselage bay panel for large transport aircraft. The plate edges in the impact test programme are clamped at the short sides into the preload fixture, which is representative of the bay panel connection to the frames with axial load introduction. The long edges are simply supported which allows possible rotation but no transverse deflection. This approximates the bay panel stringer connection, since stringers are stiff enough to constrain transverse deflection of the plate, but plate rotations at the stringer may occur.

Table 3: Estimated loads in LIBCOS panels

Material	*Lay up*	*Geometry mm L x W x T*	*Tensile loads kN*				*Compression kN*	
			0.25%	*0.4%*	*Failure*	*Dam.*	*Buckle*	*Preload*
Carbon/epoxy 977-2/HTS	A	500 x 200 x 2.125	69.9	111.9	409.0	307.7		
	A	500 x 170 x 2.125					31.7	52.2
	B	500 x 200 x 3.125	111.0	177.6	649.0	551.0		
	B	500 x 170 x 3.125					84.9	139.8
Aluminium 2024T3		500 x 200 x 2.0	73.1	117.0	172.01	146.2		
		500 x 170 x 2.0					33.0	54.4
		500 x 200 x 2.8	102.4	163.8	240.8	204.7		
		500 x 170 x 2.8					93.8	154.5

For the design of the preload test fixture and the test specimens, information is required on expected failure loads in both tension and compression. This is particularly important for load introduction into the specimen for sizing and design of suitable tabs. Table 3 summarises such calculations for longitudinal tensile and compression loads on the selected panel materials and test geometry. For the CFRP panels ply data from Cytec was used in the laminate analysis program LAP (Laminate Analysis Program) to calculate loads required for 0.25% and 0.4% tensile strains and ultimate failure load. The tensile damage load is an estimate for the case of a 30mm hole in the plate. For axial compression loads failure will be by buckling rather than compression strength failure; estimated buckling loads were based on approximate design formulae for simply supported orthotropic panels. The compression preload is calculated to be 1.4 x buckle load applied over the 200 mm wide plate.

For the design of the test specimens it is seen from Table 3 that the maximum failure load expected for undamaged carbon/epoxy plates of Lam. B is 409.0 kN, and for 2 mm aluminium it is 172.0 kN. Based on this maximum load required in the quasi-static tests to ultimate failure and using typical adhesive bond strengths, it was calculated that the 500 x 200 mm plates required tabs at least 125 mm wide for load introduction. Such tabs will also be suitable for the compression tests loaded into the postbuckling region, where loads are lower. Fig. 9 shows a typical composite plate specimen with bonded tabs. The tabs are aluminium plates 200 x 125 x 20 mm in size, each with 8 x 16 mm diameter holes bored through the thickness. They are bonded to the 750 x 200 mm composite and aluminium test plates with adhesive Epikote 02306 supplied by Hexion. They are designed to allow the same specimens to be fixed in the preload fixture (Fig. 6) for HVI testing with preload, then to be tested subsequently in the Q/S 500 kN Zwick test machine (Fig. 7) to determine ultimate

strengths. The 20 mm tab thickness is necessary to provide uniform loading across the plate width in the Q/S tests. The holes are needed to accurately locate the specimens in the preload fixture. To allow some versatility in the fixture to accommodate different plate sizes, it was convenient to have 3 rows of holes in the tabs. In the LIBCOS tests the plates are bolted to the preload fixture with bolts through the outer row of 3 holes. The remaining 5 boltholes are not required so that the composite plate is not bored through in these locations. For the Q/S tests it was found that the 100 mm diameter cylindrical heads in the machine could be clamped onto the tabs without through-thickness bolts, so that load introduction to the plate specimens was controlled by the adhesive bond shear strength.

Figure 9: Plate specimen with aluminium tabs

3.3 Test methodology

Incoming inspection

Plates are numbered according to the following scheme: Xnnn or XPnnn, where

- X may be C for composites or A for aluminium, P stands for pre-screening (P is left out if the test plate is tested in the main test program),
- nnn is a unique identifying number between 001 and 999

As the composite plates have been cut from different batches, they have a second identifying number, which is sometimes written in the middle of the back face (without “C” or “CP” at the beginning) of the test plate. This number identifies the location of this test plate in the original manufactured panel before cutting (see example in annex B, the test CP009 plate is also identified by number 1 on the back side – This can be seen in the lock-in thermography inspection).

All these pieces of information are also present in the monitoring sheet of each plate, which is accompanying the test plates for all tests and NDT inspections and in which the test/NDT engineers are writing their comments.

The incoming inspection comprises a visual inspection and a lock-in thermography investigation (only for composite plates).

In the visual inspection, following points are assessed for the composite plates:

1. The thickness of the plates is measured at four points situated 250 mm away from the small side and about 20 mm from the long side of the test plates using an indicating calliper.
2. The surface appearance of the test plates is examined. Especially colour variations, accumulations of resin, dry zones and areas, where plies may have slipped, are identified if any.
3. A tap test is conducted. The aim is to identify any difference in sound through tap testing in the test plate and report it if any.

The visual inspection is passed for the composite plates if the following criteria are fulfilled:

1. Thickness is within 2.125 mm +/- 0.15 mm (thin plates) or 3.125 +/-0.15 mm (thick plates) / Dry zones and accumulations of resin are not accepted.
2. If slipped plies are observed, there should be a gap or an overlap of less than 5 mm.

In the visual inspection, following points are assessed for the aluminium plates:

1. The thickness of the plates is measured at four points situated 250 mm away from the small side and about 20 mm from the long side of the test plates using an indicating calliper.
2. The aluminium plate should be perfectly flat.

The lock-in thermography inspection should detect any pre-damage in the test plates. The incoming inspection is passed when the visual inspection is passed according to the criteria mentioned before and if the lock-in thermography does not detect any pre-damage.

High velocity impact test

In the pre-stress fixture described in §2.2, the plates are fully clamped at the tabs whereas their lateral sides are laterally supported by lateral 420 mm long rails as shown in Fig. 10. For each plate, the lateral rails are translated so that they contact and support the test plate. The pre-loading is introduced by a hydraulic jack and is differently controlled depending on compression or tension pre-load. If the pre-loading is under tension, the level of pre-loading is controlled by four strain gauges (Figure 11). If the pre-loading is under compression in the post-buckling region the strain gauges may not be used due to the local bending in the plates. In this case the level of pre-loading is controlled by the applied compression force determined from the pressure level in the hydraulic jack. First the Q/S test on an undamaged plate was used to measure the initial buckling load Pb for the plates. As discussed in § 4.2 it was decided to apply preloads of 1.4 Pb for composite plates and 1.5 Pb for aluminium plates. After calibrating the hydraulic jack pressures in the cylinder against the resulting loads, it was then possible to determine the applied pressure for the required compression loads.

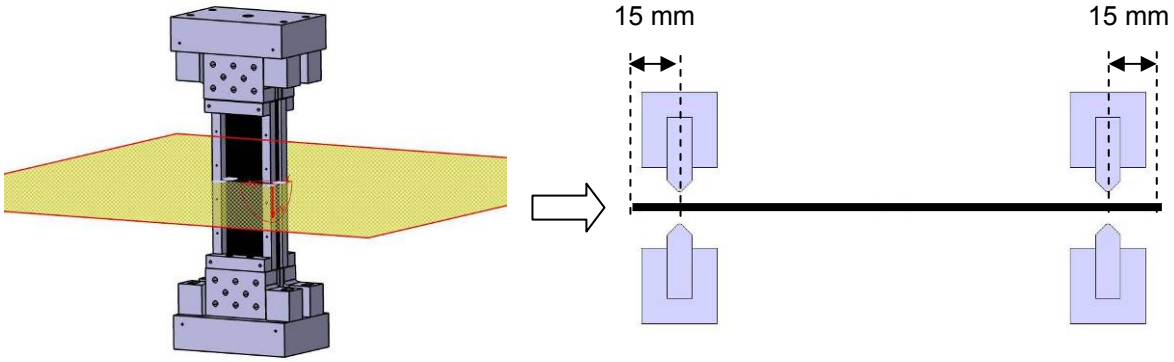

Figure 10: Principle of lateral support through lateral rails

Whatever the type of pre-loading, the test plates are equipped with four longitudinal strain gauges of type FLA-6-11-1L (produced by Tokyo Sokki Kenkyujo Co., Ltd.): two on each side (Fig. 11). These latter are located so that they cannot be damaged during the high velocity impact test. Aim is to control the uniform distribution of the strains in the test plate when preloaded under tension and to detect buckling when pre-loaded under compression.

During the high velocity impact test, a high speed film of the impact event and the signals of the strain gauges are recorded. In addition, the impact velocity of the projectile is measured through a light barrier. The camera speed is set to 30000 full frames per second with 256 x 256 pixels as resolution. The frequency of data acquisition for the strain gauges is set to 10000 Hz.

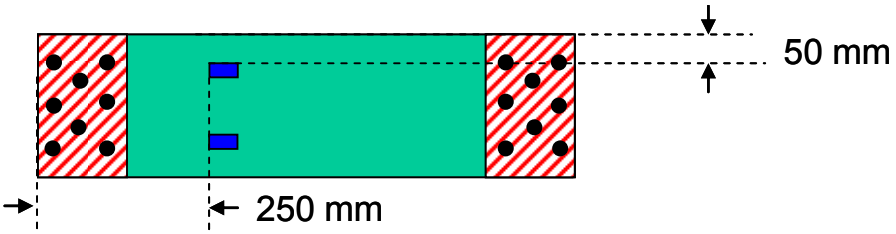

Figure 11: Position of the strain gauges on the test specimens

Lock-in thermography inspection

After the high velocity impact test, the damage in the test plate is examined through lock-in thermography. Both faces are inspected in order to determine the extent of the delamination For all the plates, a frequence of 0.05Hz is used. Based on this inspection, the delamination area may be quantified.

Residual strength test:

The residual strength tests are conducted in a servo-hydraulic universal-axial testing machine of type Zwick 1494. When the tests are conducted under tension, the signals of the strain gauges is used to control that the strain distribution is uniform. In the case of a residual strength test conducted on an undamaged test plate, a fifth strain gauge of type rosette (produced by Tokyo Sokki Kenkyujo Co., Ltd.) is added in the centre of the plate to detect the initiation of buckling during loading. This method was used to establish Pb (initial buckling load) for the composite and aluminium plates. All the signals of the strain gauges, the applied loads and the displacement are recorded during the quasi-static test. The frequency of data acquisition is set to 50 Hz.

For the residual strength tests in tension, the long side of the test plate are not supported: the pairs of rails used for the high velocity impact tests are not used. The available clampings with a diameter of 100 mm are introducing the load at the tabs. As seen in the tests, the 200 mm wide and 20 mm thick tabs are able to assure a uniform loading in the test plate.

For the residual strength tests in compression, the long sides of the test plates are supported by two pairs of 420 mm long rails built into the Q/S testing machine with knife edge contact at the plates (Fig. 12). The boundary conditions are then the same for the high velocity impact tests and the residual strength tests.

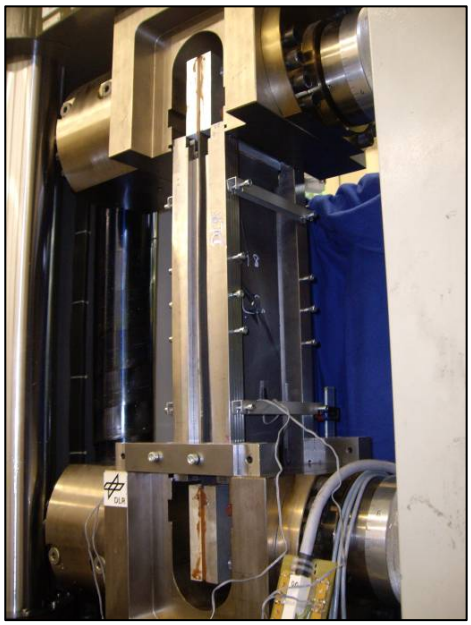

Figure 12: clamping and side support of the test plate in the QS testing machine

For some residual strength tests, the surface of the test plate is painted in white then black spots are sprayed. Aim is to digitize the displacement field during the testing and derive the deformations of the test plate with the **GOM system** at various load levels if wished.

4 Results from preliminary test programme

4.1 Test plan and pre-test matrix

The main objective of LIBCOS is to carry out a systematic experimental test programme of gas gun impact tests with selected projectiles on representative aircraft carbon composite panels under both tension and compression preloads: both notch damage and delamination damage should be investigated. The panels to be tested were described in §3 above based on transport aircraft materials and typical fuselage bay panel geometries. As discussed in the introduction it follows from the damage tolerance requirements that Category 1 (barely visible impact damage, BVID) is based on a *no-growth* concept, meaning that damages up to the boundary of visible detectability, will not grow under operational loads (DLL) and will not cause a loss of the residual strength below design ultimate load level (DUL). Category 2 and 3 are visible impact damage (VID) seen in routine and visual inspections. Here the residual strength may not fall below limit load level (DLL) corresponding to maximum operational load cases. Thus the appropriate preload levels for the LIBCOS test plates are typical DLL conditions, and the main interest is to study the dependence of impact damage and residual strength after impact on preload levels.

After study of aircraft design guidelines and discussions with Airbus it was decided that tension preloads of 0.15% strain and 0.25 % strain are appropriate, which correspond to DLL for aircraft composite shell structures. This will be applied as a longitudinal tensile strain along the major plate axis. Note that biaxial strains are not possible in the current design of the preload fixture. Compression preloads causing panel buckling were discussed with Airbus and also EASA. It was decided in LIBCOS to apply an axial compressive preload in the unbuckled and post-buckling range. A composite fuselage bay panel may buckle at DLL, particularly as buckle loads cannot be precisely defined in real structures due to the strong influence of geometric imperfections. An initial Q/S test on an undamaged panel was carried out to determine buckling load Pb. Then the maximum compression preload was selected to be 0.5 Pb (unbuckled) and 1.4 Pb (buckled) for the composite panels, similarly 1.5 Pb for aluminium panels. Note that at buckling failure the aluminium panels deform plastically and retain a load carrying ability, whilst the CFRP panels fail by brittle fracture, thus higher compression preloads could be considered for the aluminium panels.

The choice of impact scenario (impactor type, mass, velocity) is supported by HVI tests on composite panels and previous impact simulation studies at the DLR and in the literature on composite and metallic plates to assess expected damage. DLR experience has shown that impacts with hard bodies such as metal debris causes fibre fracture and penetration in composites, whilst soft bodies such as gelatine bird, ice and tyre rubber cause delamination damage without significant penetration. Blunt impactors, such as stone, concrete or glass balls may lead to penetration or delamination, depending on velocities and panel thicknesses. Thus it is important for the study to include both hard metal and blunt projectiles to generate different types of damage. The impact scenarios were left unspecified at the LIBCOS KO meeting and it was agreed that impactors and impact velocities will be fixed after a small pre-test campaign on loaded and unloaded plates. The priorities for this limited testing were to understand the relative behaviour of loaded and unloaded composite structure when subjected to impacts which result in several key failure modes, i.e. notch damage and delamination. Although the use of directly defined regulatory threats would have been preferred, the limitations associated with this work package required some compromise.

Thus the main purpose of the pre-screening tests is to define precisely the impact test scenarios and preload levels for the main test LIBCOS programme, and to verify appropriate test conditions related to specimen geometry, specimen preparation, support conditions and instrumentation. Possible preload conditions and impact scenarios are summarised in the

pre-screening test matrix Table 4. For the pre-screening tests in compression, loads were applied in the buckling range, which is expected to be the more extreme case. The unbuckled compression load case is included in the main test programme. For notch damage impact, tests were carried out with 100 g steel beams, dimensions 108 mm x 30 mm x 4 mm, and 12 mm steel cubes with mass 13 – 14 g. For delamination/indentation damage tests were performed with a 100g rubber beam, dimensions 134 mm x 30 mm x 24 mm, and as blunt impactors glass balls diameter 24 mm, mass 18 g. After impact the damage to the composite plates was quantified using lock-in thermography, before Q/S tests were performed on the same tabbed plates to ultimate failure to establish residual strength of the damaged plates. Q/S tests of undamaged plates in tension and compression were carried out to establish baseline tensile and compression ultimate loads.

Table 4: Impact pre-test matrix for composite (C) and aluminium (A) plates

Impact scenarios		Compression preload		Tension preload		
Prestrain:		C: 1.4 Pb A: 1.5 Pb	0	0	+0.15%	+0.25%
Notch damage	Vel. 1	X	X	X	X	X
Delamination/ indentation	Vel. 2	X	X	X	X	X

4.2 Summary of test results

The pre-screening test results are summarised in Annex A, Tables A1 – A3. As reference point, note that pre-screening test plates are numbered in series CP00x for composites, and AP00x for aluminium. In the subsequent main test programme, the plate specimens are numbered C00x, A00x for composite and aluminium, respectively. The numbering sequence x, … continues from the pre-screening to the main test programme. The tables list the impact test case with projectile type, mass, impact velocity and impact energy. Residual strength data after the post-impact quasi-static tests are listed, together with the *residual strength factor (RSF)*. This is defined as:

RSF = failure load in damaged plate / failure load in baseline (undamaged) plate.

This factor provides a quick assessment of the effect of impact and preload on residual strengths. As reference, details of impact damage from thermography and post-test photos are shown in Annex B (composites) and Annex C (aluminium) for each plate tested in a numbered sequence.

Composites with tension preload
Table A1 summarises the impact and residual strength tests on the 2.1 mm thick composite plates CP001 – CP009 under tensile loads, and impact from steel beams, steel cubes, a rubber beam and glass balls. The measured load-displacement curves for the plates up to failure are shown in Fig. 13. Plates CP001 and CP007 were used for determination of baseline tensile strength under Q/S tensile loads, without impact damage. Test CP001 failed in the tabs at a load 221.8 kN which was well below the 409 kN predicted from laminate theory in Table 4. This led to the redesign of the tabs and bonding system. The use of the 8 bolts per tab was stopped, as they caused stress concentrations, and in subsequent tests

only the 3 outside bolts were used, which was the minimum required for stabilising the plates in the preload fixture. The initial epoxy resin was also changed to a more ductile resin system Epikote 02306. The bonding was investigated with CP007, which was cut into two 100 mm wide plate specimens: CP007a with the ductile resin system; CP007b with GRP inserts between the aluminium tabs and the composite plate. Specimen CP007a failed in the composite gauge length at 217.8 kN, whilst CP007b failed at the tab interface with load 195.6 kN, see test curves in Fig. 13 and photos of fractured specimens in Annex B. This confirmed that the ductile adhesive was the best solution for bonding the aluminium tabs to the composite specimens, and extrapolation to a 200 mm wide specimen gives a baseline tensile strength value of 435.6 kN, which is about 6% above the CLT prediction. The ductile adhesive was used in subsequent tests, together with 3 outer transverse bolts per tab.

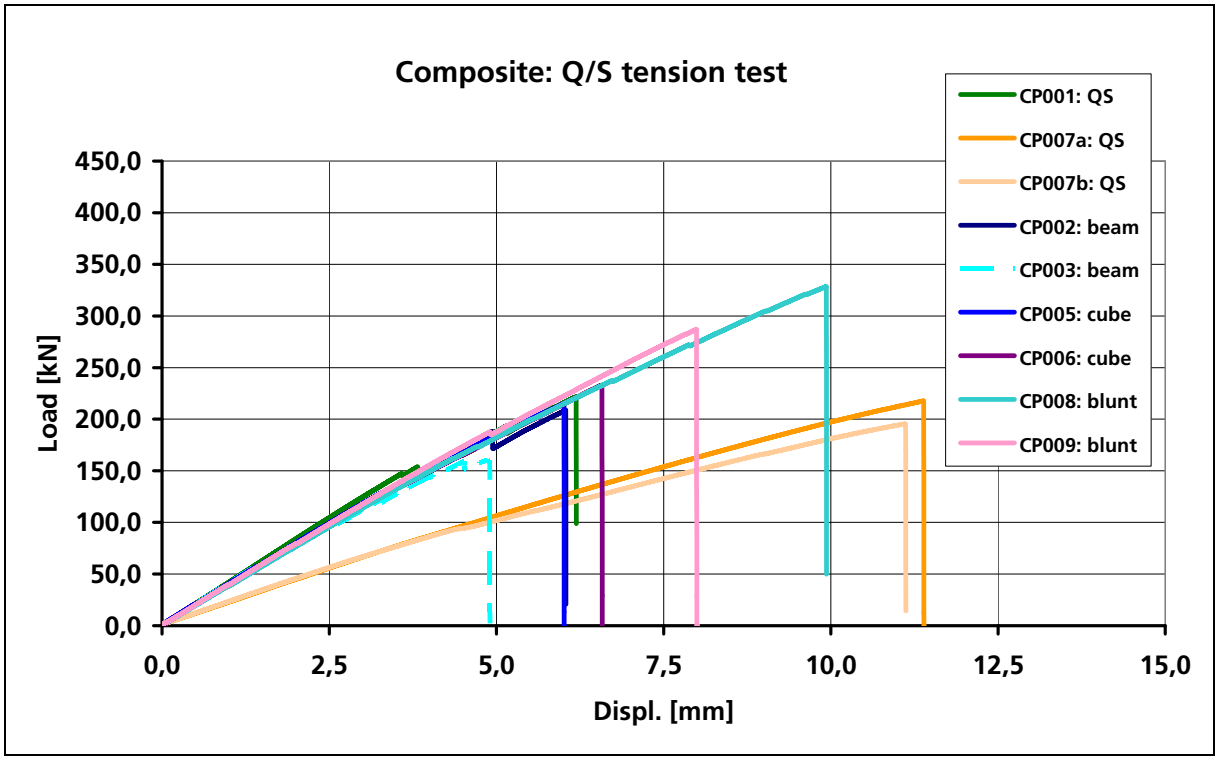

*broken curve indicates no preload

Figure 13: Residual strength test data for 2.1 mm composite plates in tension

The pre-screening composites plate tests with tension preload showed that the pre-load fixture works very well, with pre-loads controlled and monitored by the 4 strain gauges attached to the plates. In the Q/S tests after impact with damage the load-deflection curves were almost linear up to an 'explosive' brittle failure as seen in Fig. 13, with final failure initiated from the central notch or delamination damage. Notch damage was observed from the steel beam and steel cube impact tests at velocities in the range 63.9 – 103.7 m/s. RSF factors of 0.37 and 0.48 were measured for steel beams, whilst notch damage from the cubes led to RSF values of 0.49 and 0.53, which are significant reductions as required in the test programme. The pre-tests showed clearly that required notch damage could be achieved with the 12 mm steel cubes at impact velocities above 65 m/s, see curves for CP002 and CP005 in Fig. 13 which were almost coincident. The steel cubes are preferable to the larger 100 mm steel beams, which cause large unrepresentative damage in these 200 mm wide plate specimens. However, the steel cubes were not very reliable for delamination damage at lower velocities, as test CP006 shows in which rebound occurs, but the sharp metal edges of the cube led to surface fracture and penetration on the front face with delamination at the rear face. The result is then similar to notch damage.

Test CP004 (not shown in Fig. 13) with the 100 gram tyre rubber beam at 99 m/s (497 J) caused no detectable delamination damage in the plate, despite the high impact energy. The

trial tests with 24 mm diameter glass balls (CP008, CP009) caused extensive delamination at the back face of the plates, without fibre fracture or penetration. This was confirmed by the thermography results shown for each plate in Annex B. RSF of 0.66 and 0.75 are also significant reduction factors for this test programme. Subsequent tests in the compression programme with glass balls showed good reproducibility in delamination damage area. For this reason it was proposed for the blunt impact delamination damage case to concentrate on glass ball projectiles in the main test programme. As an impact scenario this corresponds to stone or concrete runway debris damage, which is relevant to both fuselage and wing panels.

In the pre-tests the only case in which there are RSF data with and without tensile preload for the same impact conditions are plates CP002 and CP003. Here it is seen that there is more impact damage and a lower RSF without tensile preload. However, little can be concluded from a single test. To avoid spurious results due to scatter in plate properties and differences in the impact conditions between tests, it was decided in the main test programme that there should where possible be 3 repeat tests for each impact case. Although not statistically significant, this was considered to be a necessary compromise within the limited bounds of the time and resource available for this investigation.

Composites with compression preload

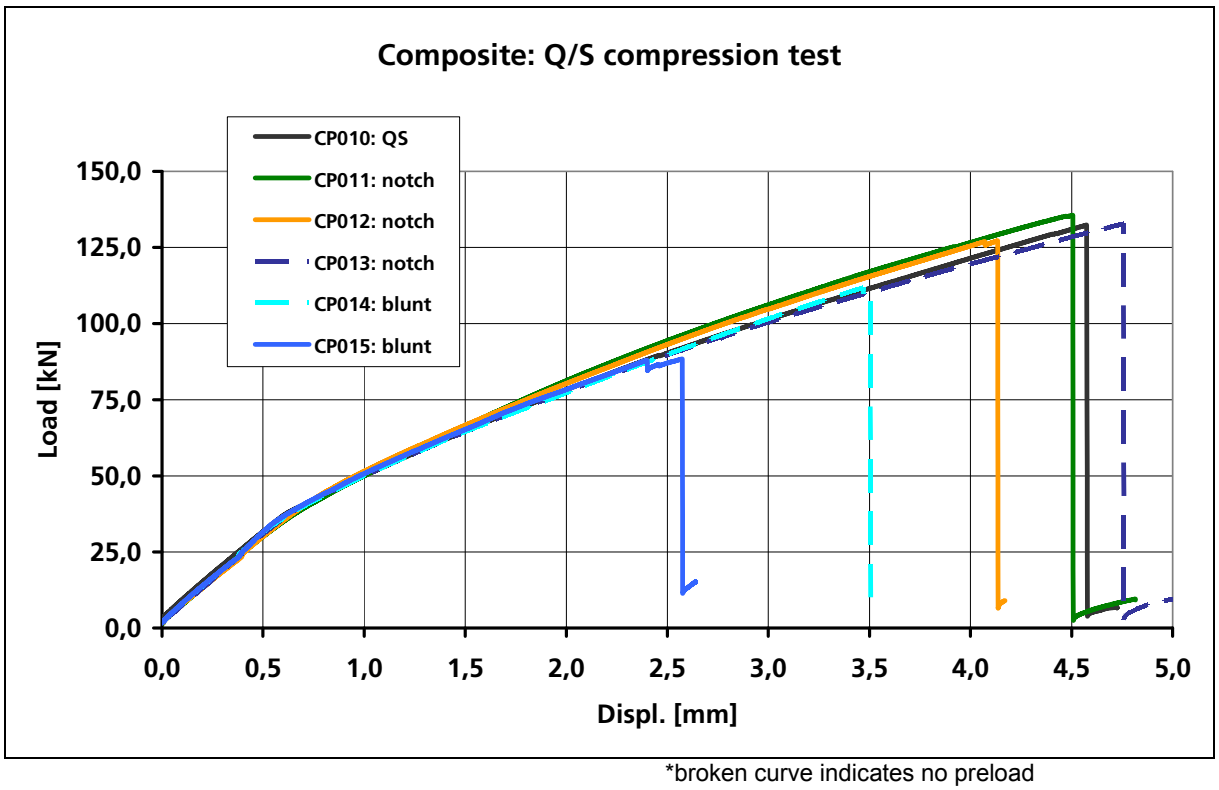

*broken curve indicates no preload

Figure 14: Residual strength test data for 3.1 mm composite plates in compression

Table A2 summarises the pre-screening tests with 3.1 mm thick composite plates in compression CP010 – CP015, with the corresponding load-deflection curves shown in Fig. 14. Test CP010 was the Q/S test in compression with lateral supports to determine buckling load, mode of buckling and compression ultimate load. The plate had 7 strain gauges in total and it was verified that monitoring the strains in the 4 standard strain gauges positioned 250 mm from the plate lower edge showed a clear bifurcation in surface strains, which indicated the buckling point. This corresponded to an axial compression load of ~ 38 kN. Ultimate failure was at 132.4 kN with maximum axial displacement 4.6 mm, which corresponds to an ‘effective’ compression strain at failure of 0.92% on the 500 mm plate length. Note that the measured buckling load was much lower than the 84.9 kN predicted in

Table 4, which is commonly observed in buckling tests due to plate imperfections and non-ideal boundary conditions. In all pre-screening compression tests the plate buckled into 3 longitudinal cell buckles and the impacted face was convex at the central impact point.

For the HVI tests with preload it was decided to load into the buckling region, where it was assumed Pb = 38 kN from the undamaged plate test. Due to the low buckle load, it is assumed that the plates in an aircraft structure will be in the postbuckle region at design LL. Thus applied compression preloads were usually applied in the range 0.95 Pb - 1.4 Pb, which corresponds to LL in compression. The hydraulic jack in the pre-stress fixture was calibrated and for the compression tests with preload, loads of 53.2 kN were applied, which corresponds to 55 bar pressure in the jack. It should be noted from these tests that the Q/S buckling load is not a constant for these panels, and is influenced by plate imperfections and small differences in support conditions. Thus test CP012 which was loaded to 0.95 Pb, was still in a light buckled state in the preload fixture due to its very high length/thickness ratio.

Impactors were the 12 mm steel cube which at the impact velocities chosen 134.0 – 135.9 m/s caused notch failure, with extensive delamination and ply damage at the rear face, as seen by the post impact test photos in Annex B. For the tests without compression preload a small load of 2 - 5 kN was applied to stabilise the plate in the impact test fixture. After impact there was significant notch damage in the plates as the cubes passed through. The thermography images in Annex B show that the damage extends to the plate edge supports. In the Q/S residual strength tests the plates adopted the same 3–cell buckled shape. Fig. 14 shows that all plates, including those with extensive notch damage, had the same initial stiffness properties, and all buckled at about the same point (~0.6 mm displacement, ~ 38 kN). After initial buckling the buckle amplitude increased significantly, as seen by the nonlinearity in the test curves, however, even with notch damage the continued buckling and final collapse load were not significantly reduced by notch damage, see curves CP011, CP012, CP013. The RSF values were in the range 0.96 – 1.02 showing that the significant notch damage does not influence the buckling failure strength of the plates which is an unexpected result.

CP014, CP015 were blunt impact tests with glass balls to initiate delamination damage. Here there was little or no visible damage on the front face, with some splitting of the rear 45° plies on the back surface, see Annex B. The thermography images show however large delamination regions around the impact position. Fig. 14 clearly shows that these plates fail earlier than those with notch damage and for these tests RSF values of 0.67 - 0.84 indicate a more significant residual strength reduction. The first results are interesting as they show for the preloaded plate CP015 a significantly lower failure load than CP014 without compression preload. This effect is probably related to the large delamination areas in the centre of the plate. This will be investigated further in the main test programme, where attention is given to the compression pre-load level by additional tests with lower compression pre-load 0.5 Pb in the unbuckled range before impact.

Aluminium with tension preload

Pre-screening tests on 2 aluminium plates with tensile loads are summarised in Table A3 with measured load-deflection curves shown in Fig. 15. AP001 was the baseline test on an undamaged 2 mm plate, which showed an initial elastic response, with onset of yield and plastic flow at about 4 mm displacement and load 155 kN. There was then steady plastic flow until ultimate failure at an extension of 34 mm and load 182.5 kN. Note this is well below the ultimate load of 2.1 mm composite plates at 435.6 kN. However, the relative sizing of the aluminium with respect to the composite was only approximate, the relative behaviour of unloaded and preloaded structure made from each material being of more interest. Test AP002 had 0.23% tensile prestrain, with steel beam impact which caused a large notch damage about 30 mm in size. In the Q/S residual strength test 2 main cracks initiated at the notch and propagated transverse to the plate, leading to brittle failure at about 4 mm

extension and load 138.4 mm and giving a residual strength factor of 0.76. Fig. 15 shows the marked notch sensitivity of aluminium plates compared to undamaged plates. This is a higher RSF than those measured in the 2.1 mm composite plates, however the failure loads were still higher in the notched composite plates, due to their better tensile strength properties.

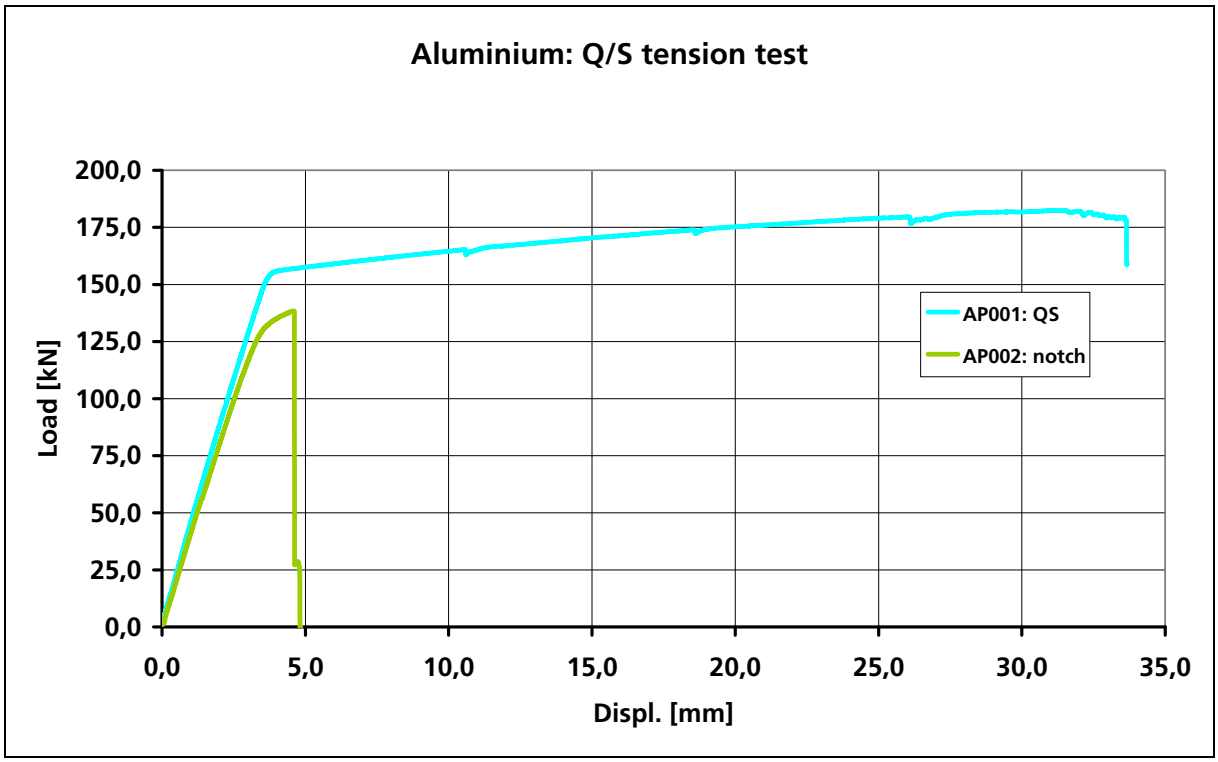

Figure 15: Residual strength test data for 2.0 mm aluminium plates in tension

Aluminium with compression preload

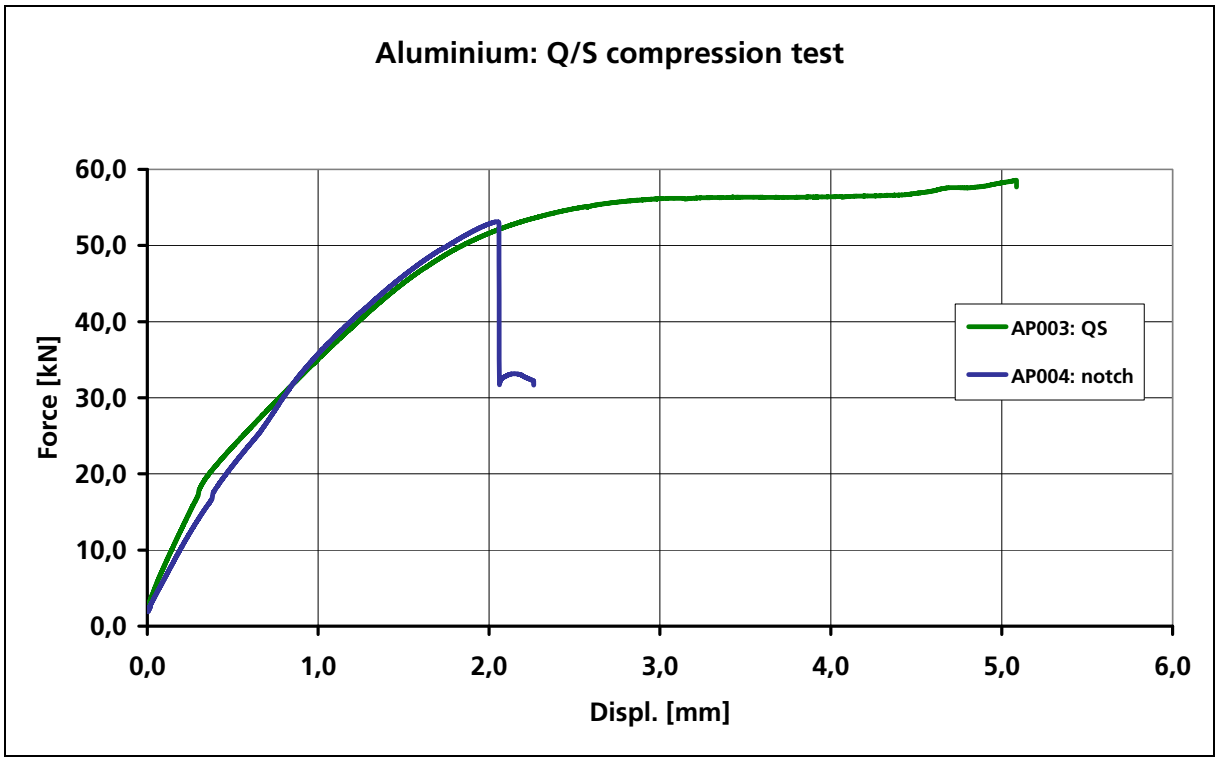

Figure 16: Residual strength test data for 2.0 mm aluminium plates in compression

In the compression programme AP003 was tested in Q/S compression to determine buckling mode, again 3 cell buckles, and buckling load of about 20 kN, see Fig. 16. On further loading the buckles increased in size with extensive plastic deformation, but the panel did not fracture and tests were stopped at 5 mm displacement, and maximum loads of 58.6 kN. Plate AP004 was impacted by the 12 mm steel cube with a preload 1.5 Pb giving extensive notch damage. Compression tests into the postbuckling region did not lead to fracture but buckling and plastic flow. At a load of 53 kN the plate buckled prematurely in the 40 mm space between the tab and end of the lateral support rails. The test was stopped at 2.1 mm displacement with maximum load 53 kN. This corresponds to an RSF value 0.93 indicating that plate buckling failure loads are not strongly influenced by notch impact damage. However the high notch sensitivity of aluminium is seen by the much lower extensibility due to the notch. As a result of the early failure in a small unsupported part of the plate edges, it was decided that the edge support rails should be extended for subsequent tests. This minor change to the support fixture was made and the extended supports used for both compression preloads and residual strength tests.

4.3 Discussion of results

Table 5: Residual strength factors (RSF) from pre-screening test programme

	Loading	**Preload**	**RSF: Notch impact damage**	**RSF: Delamination/ indent damage**
Composite tests plates	Tension	0 0.25 % strain	0.37 0.48 – 0.53	TBD 0.66 – 0.75
	Compression	0 0.95Pb - 1.4Pb	1.0 0.96 – 1.02	0.84 0.67
Aluminium test plates	Tension	0 0.25 % strain	TBD 0.76	TBD TBD
	Compression	0 1.5 Pb	TBD 0.93	TBD TBD

The purpose of the pre-screening test programme was to establish impact and preload conditions for detailed study in the main test programme. Thus no detailed analysis of the test data and the study of the influence of preload and impact damage on residual strengths is carried out at this point as there are insufficient data to make conclusions. A brief overview of the residual strength factors (RSF) taken from Tables A1 – A3 in Annex A is given in Table 5. As expected the effects of impact damage and preload have different significance for composite plates, compared to aluminium The table shows that composite plates with tension preload and notch damage have the lowest RSF values 0.37 – 0.53; with delamination damage, RSF are also significantly reduced in the range 0.66 – 0.75. The aluminium plate tested had a corresponding RSF of 0.76 for notch damage, indicating that the composite plates are more sensitive to impact damage than similar sized aluminium plates. However, the absolute tensile strength values of the composite plates are higher than the damaged aluminium plate due to higher baseline (undamaged) tensile strengths for composite, see Tables A1 – A3 for details.

For composite plates with notch damage RSF values were 1.0, without preloads, and 0.96 – 1.02, with 1.4 Pb preloads. The results for compression preload are unexpected in that preloading into the post-buckling region did not significantly reduce compression buckling ultimate failure loads, even when there was significant notch damage. However delamination

damage, which was often barely visible on the impacted face, caused higher ultimate strength reductions, with RSF of 0.84 without preload, and 0.67 with buckling preload. These are interesting preliminary results which now require confirmation from more detailed study in the main test programme. They underline that BVID rather than visible notch damage in plates penetrated by steel cubes are of more concern for compression loaded panels. For the aluminium plate under compression buckling, RSF was 0.93 for notch damage with buckling preload, indicating that these combined effects are not very significant in aluminium panels.

Discussion of the pre-screening tests with EASA led to a clear concept for the main test programme. This will focus on two impact scenarios causing notch damage (with plate penetration or through-thickness cracks) or blunt impact damage with no visible cracks but delamination damage in composites or plastic indentation in aluminium. Both types of damage will be investigated in plates subjected to both tension and compression preloads. More emphasis will be given to composite plates, with a greater number of tests, compared to aluminium. Based on this the main test plan was defined, and is summarised in Tables 6 - 9 below, with further discussion in § 5.1. The pre-screening tests also emphasised the importance of NDE in evaluating impact damage in composite plates. This is because there was not a clear correlation between visible impact damage and residual strengths; it was significant in the notch tests in tension, but in the blunt impact tests there was almost no visible damage on the outside of the plates, yet RSF were also reduced in both tension and compression. It is thus important in the main programme that NDE is carried out on all impacted composite plates, before Q/S tests to measure residual strength. The pre-screening tests showed that thermography is appropriate since tests are fast and plates require no special preparation. Damage surfaces are not so clearly defined with thermography in comparison with ultrasonic C-scan and certain judgement is required for good evaluation. However use of standard C-scan where plates are scanned in a water tank and must then be dried before Q/S strength tests was considered to be too time-consuming in the current investigation.

5 Results from main test programme

5.1 Main test plan

The main test programme has been planned to examine in detail the tendencies seen in the pre-screening tests. It is split into four parts as indicated in Tables 6 – 9. For composites it is proposed to use the 12 mm steel cubes for notch damage and the 24 mm glass balls for blunt impact tests leading to delamination damage, with velocities adjusted by the plate thicknesses to give the required failure modes in tension and compression cases. Suitable impact velocities have been established by the pre-screening tests. The preliminary test results indicate that for composites there is a large strength reduction from notch damage under tensile loads, which is expected. However in the post-buckling region of compression loads this damage does not lower the RSF. In this case barely visible delamination damage from lower energy blunt impact tests leads to more significant strength reductions. Particular attention will be given to this case in the main test programme. The steel cubes were shown to give notch damage in aluminium plates, so that similar impact scenarios for notch damage can be used for aluminium and composite plates. Tensile preloads will be up to 0.25% strain for both composite and aluminium plates, monitored by the two pairs of back-to-back strain gauges attached to the plates.

For compression preloads axial strains in the plate are not suitable for controlling the preload levels since at strains well below 0.25% the measured strains indicate a combined compression plus plate bending strain field due to the onset of buckling in the thin plates. The quasi-static tests on undamaged plates were used to define a compression buckling load Pb for composite and aluminium plates with the same end clamping conditions and

lateral rail supports. Note that onset of buckling is strongly sensitive to plate specimen due to geometrical imperfections and exact clamping and support conditions, thus the measured Pb values are not constant and are used as a guideline for the test programme. After discussion with EASA it was decided in the main programme to apply compression preloads in the post-buckle range of 1.4 Pb for composite and 1.5 Pb for aluminium, together with preloads of 0.5 Pb in the unbuckled state. Due to the limited resources, it is not considered necessary to consider aluminium plates impacted in the unbuckled state in the main programme. Indentation damage in aluminium is most probably of secondary importance. A few such tests are included in the final test matrix to check this phenomenon.

The main programme will allow a detailed analysis of impact damage and preloads on composite and aluminium plates. It was agreed with EASA to fix where possible the impact conditions, projectile, mass, velocity and hence kinetic energy for each of the four main impact scenarios (tension/compression preloads, notch/blunt impact damage) and where possible to carry out 3 repeat tests for each load case. In this way it is hoped to confirm trends of behaviour. Due to the limited number of plate specimens, it is not therefore possible to study other parameters such as the role of increasing energy for each scenario. The importance of delamination damage after impact is being evaluated quantitatively by measuring the delamination area observed in the thermography tests and correlating this with the impact energy and RSF values. For the aluminium plates notch size will be measured after impact to see how this correlates with RSF values. In this way it is intended to correlate plate residual strengths with size and type of damage, obtained by visual inspection and NDE, which could allow the conclusions to be used more widely for damage tolerance assessment under a wider range of impact conditions.

The main test matrix is proposed in Tables 6 -9. Note that in addition to the new test campaign, it was decided to include selected pre-screening results in the later evaluation. These are added into the test matrix here for reference. The previous data are included only when the test conditions are within the envelope defined for the main test programme.

Table 6: Composite plates: 2.1 mm thick with tension preload

Load cases	**HVI conditions**		**Preload conditions: tensile strains**			**Q/S tensile strength test**
	Velocity m/s	**Energy J**	**0**	**0.15 %**	**0.25 %**	
Baseline strength no damage	N/A	N/A	N/A	N/A	N/A	2 tests + CP07a
Notch damage 12 mm steel cube (13 g)	~ 100	~ 65	4 tests	1 test [1]	3 tests + CP005	8 tests
Delamination damage 24 mm glass ball (20 g)	~ 65	~ 40	4 tests	1 test [1]	2 tests + CP008, CP009	7 tests

[1] Tests with 0.15 % strain were reduced to 1, to check the effect, thus allowing resources for extra HVI tests in the unbuckled compression state (Table 6).

Table 7: Composite plates: 3.1 mm thick with compression preload

Load cases	HVI conditions		Preload conditions: compression loads			Q/S compression strength and buckle loads
	Velocity m/s	Energy J	0	0.5 Pb	1.4 Pb	
Baseline strength no damage	N/A	N/A	N/A	N/A	N/A	3 tests + CP010
Notch damage 12 mm steel cube (13 g)	~ 135	~ 120	2 tests ² + CP013	3 tests	3 tests + CP011	8 tests
Delamination damage 24 mm glass ball (20 g)	~ 85	~ 75	2 tests ² + CP014	3 tests	6 tests ²	11 tests

² By adding data from pretest series, we can reduce some tests to 2 per load case, allowing 6 tests with delamination damage for convex and concave buckle impact cases.

Table 8: Aluminium plates: 2 mm thick with tension preload

Load cases	HVI conditions		Preload conditions: tensile strains		Q/S tensile strength test
	Velocity m/s	Energy J	0	0.25%	
Baseline strength no damage	N/A	N/A	N/A	N/A	1 test + AP001
Notch damage 12 mm steel cube (13 g)	~ 100	~ 65	3 tests	3 tests	6 tests
Indentation damage 20 mm steel ball (xx g)	~ 60	~ 40	1 test	1 test	2 tests

Table 9: Aluminium plates: 2 mm thick with compression preload

Load cases	HVI conditions		Preload conditions: compression loads		Q/S compression tests for buckle and maximum loads
	Velocity m/s	Energy J	0	1.5 Pb	
Baseline strength no damage	N/A	N/A	N/A	N/A	1 test + AP003
Notch damage 12 mm steel cube (13 g)	~ 100	~ 65	3 tests	3 tests + AP004	6 tests
Indentation damage 20 mm steel ball (xx g)	~ 60	~ 40	1 test	1 test	2 tests

5.2 Summary of test results

The main test results are summarised in Annex A, where the programme is divided into four main parts composites-tension, composites-compression, aluminium-tension and aluminium-compression reported in Tables A4 – A7, respectively. As stated above the plate specimens are numbered C00x, A00x for composite and aluminium, respectively. Where specimens are added from the pre-screening programme they retain their original numbers CP00x or AP00x. For each of the four test series, data are presented for the two impact scenarios, notch or blunt impact with and without pre-loads. The tables list the projectile type, mass, impact velocity and impact energy. Residual strength data after the post-impact quasi-static tests are given, together with the *residual strength factor (RSF)*, defined as the ratio of the failure load in the damaged plate to that in the undamaged baseline plate. For ease of reference the tables are colour-coded, with white representing the Q/S tests on undamaged plates to establish baseline strengths, yellow represents plates impacted with zero preload (in practise very small loads are applied to stabilise the plate in the impact frame) and pink represents plates with preload. Detailed reference information on each plate specimen is provided in Annex B, listed in a numbered sequence. These sheets show impact damage from thermography and post-test photos for each plate tested.

Quasi-static baseline tests

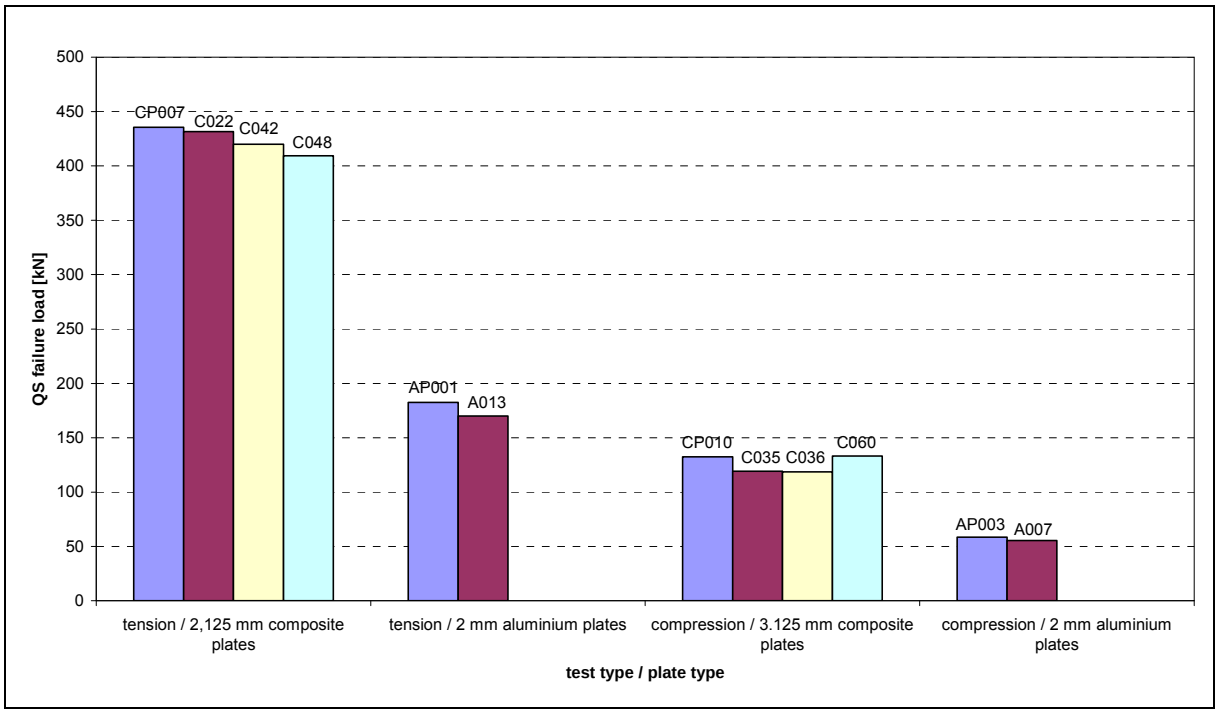

Figure 17: Baseline plate strengths measured on undamaged plates

In each of the four main plate test programmes Q/S tests were carried out on the standard 500 mm x 200 mm tabbed plate specimens to determine plate failure loads in undamaged plates. A limited number of repeat tests were performed to give some indication of inherent scatter in properties, due to the materials or plate bonding and clamping conditions. Details on the tests are given in the main results Tables A4 – A7. Fig. 17 gives an overview of the measured failure loads. It shows that for the chosen specimen materials and geometries in LIBCOS the composite plates have tension and compression failure loads generally about twice as high as those measured in the aluminium plates. It confirms also that plate compression strengths due to buckling failures are low, typically about 25% of the tensile strengths. These large differences in baseline properties should be kept in mind when working with the RSF values, which are all normalised to unity for each test series.

The figure also shows some scatter in baseline strengths, from the specimens tested. In the case of the composites materials, the test plates were cut out of larger panels which were manufactured at different times. Initial tests showed some scatter in properties from batch to batch due to manufacture and there is a small scatter in plate thicknesses as seen in the specimen pre-screening on delivery. Depending on the manufacturing batch, the thickness of the plates used for tensile preloading varied between 2 mm and 2.16 mm whereas the thickness of the plates used for compressive pre-loading was between 3.05 mm and 3.12 mm. Thus it was decided to carry out a baseline test on each batch. The tensile plates were cut from 2.1 mm thick panels panels P, B, C, D, whilst the compression plates were cut from 3.1 mm panels A, F, H. Fig. 17 indicates plate tensile failure loads in the range 409.4 – 435.6 kN for the four panels, with compression failure loads from three panels in the range 118.8 – 133.2 kN. In order to minimise this scatter in the final results analysis, it was decided to use the appropriate baseline strength values for each panel, when calculating the RSF value for the batch of plates cut from that panel. Normalised in this way, it is possible to account for both manufacturing quality and small variations in thickness from batch to batch (see §3.3). For this reason, the panel ID letter for the composite panels is listed in tables A4 and A5 with the plate ID number. For the aluminium plates two baseline tests were carried out in tension and compression, indicating a small variation in strengths. In this case the mean tensile and compression strengths are used for the RSF values, as all aluminium plates were cut from a single manufactured panel and materials variability is not anticipated.

Composites with tension preload

Table A4 summarises the impact and residual strength tests on the 2.1 mm thick composite plates. In total 23 plates were used in the main composites-tension programme, including 4 baseline plates, 10 plates subjected to impact from 12 mm steel cubes at velocities causing penetration with notch damage, and 9 plates subjected to blunt body impact from 25 mm diameter glass balls causing delamination damage. Tension pre-load was determined by monitoring plate strains away from the central impact point, near a clamped edge, as discussed above. For the tests without preload, small strains of 0.02% were applied to hold the plate in the loading frame. Preloads of 0.25% longitudinal strain were applied for the main test series with notch and blunt impact, with just one test at 0.15% strain for each case.

The measured tensile load-displacement curves up to failure for the plates with notch damage are shown in Fig. 18: The baseline curves (marked QS in this and subsequent figures) are included for comparison. Notch damage tests had impact velocities in the range 84.5 – 103.1 m/s, with kinetic energies 47.9 – 71.2 J. All plates with notch impact damage had visible damage where the cube passed through the impacted face, with extensive damage and delamination at the back face. In the residual strength tests the impacted plates with notch damage exhibited similar initial response to the baseline plates, with almost linear behaviour up to an 'explosive' brittle failure as seen in Fig. 18. Final failure initiated from the central notch and moved to the plate edges near the centre of the plate, see photos of damaged plates in Annex B. The notch damage is severe and led to failure loads equal to about half the baseline strengths, with RSF factors in the range 0.48 – 0.61.

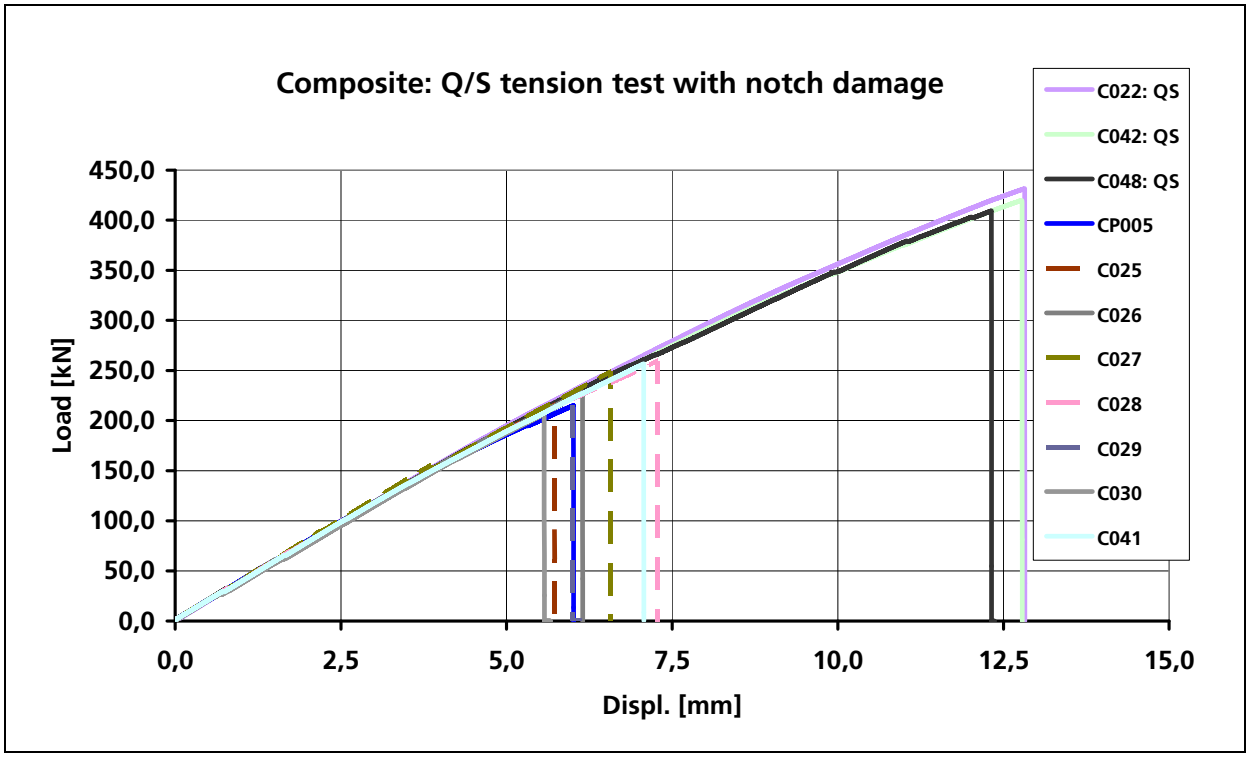

*broken curve indicates no preload

Figure 18: Tensile test curves for 2.1 mm composite plates with notch damage

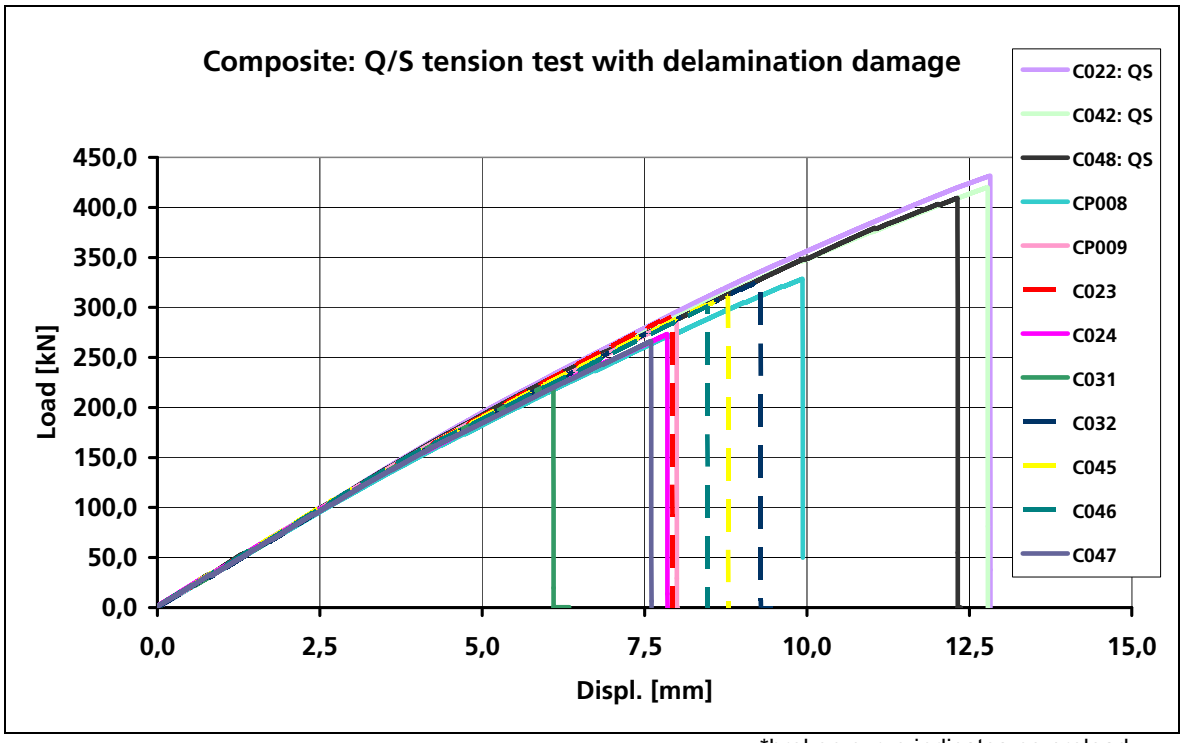

*broken curve indicates no preload

Figure 19: Tensile test curves for 2.1 mm composite plates with blunt impact damage

The measured tensile load-displacement curves up to failure for the plates with blunt impact damage are shown in Fig. 19, together with the baseline curves. The blunt impact tests with the 25 mm glass balls had impact velocities in the range 63.8 – 69.7 m/s, with kinetic energies 36.6 – 51.0 J. In all cases the plates had a small round contact mark on the impact face, with light delamination of the outer 45° ply visible on the back face. However, the thermography tests indicated extensive delamination damage near the back face. In the residual strength tests with delamination damage the test curves deviated a little from the baseline curves as the damage propagated, and again failed with an 'explosive' brittle facture. Final failure surface showed extensive fibre and ply pull-out over the complete plate width, see photos of damaged plates in Annex B. The delamination damage caused significant reduction in tensile failure loads, which was unexpected, with RSF factors in the range 0.63 – 0.76. One test C031 at 0.15% prestrain had a low RSF value of 0.52, in the range of the notch damage tests.

Fig. 20 provides an overview of the RSF values from tensile tests on the 2.1 mm composite plates, with notch and blunt impact damage. It shows clearly the magnitude of the tensile strength reductions due to notch and blunt impact damage. It shows that for blunt impact there is a clear tendency for a small reduction in RSF with preload with mean RSF values reduced by about 10% from 0.73 without preload to 0.67 with 0.25% strain preload. For notch damage the influence of preload is not so strong, mean values without preload are 0.56 and with 0.25% strain preload, they are 0.52, which is about 7% lower. However these effects could be within the scatter band of the results. It should be remembered for the notch damage tests that the projectile is a steel cube. Study of the HS film of the tests shows that first contact at impact may be flat contact from the cube face, line contact from an edge, or point contact from a corner. Experience has shown that point and edge contacts are more likely to cause directly notch damage and penetration, whilst face contact may lead to rebound. It follows that more scatter in behaviour is expected for impact damage and hence residual strength with steel cubes, compared with blunt spherical impactors.

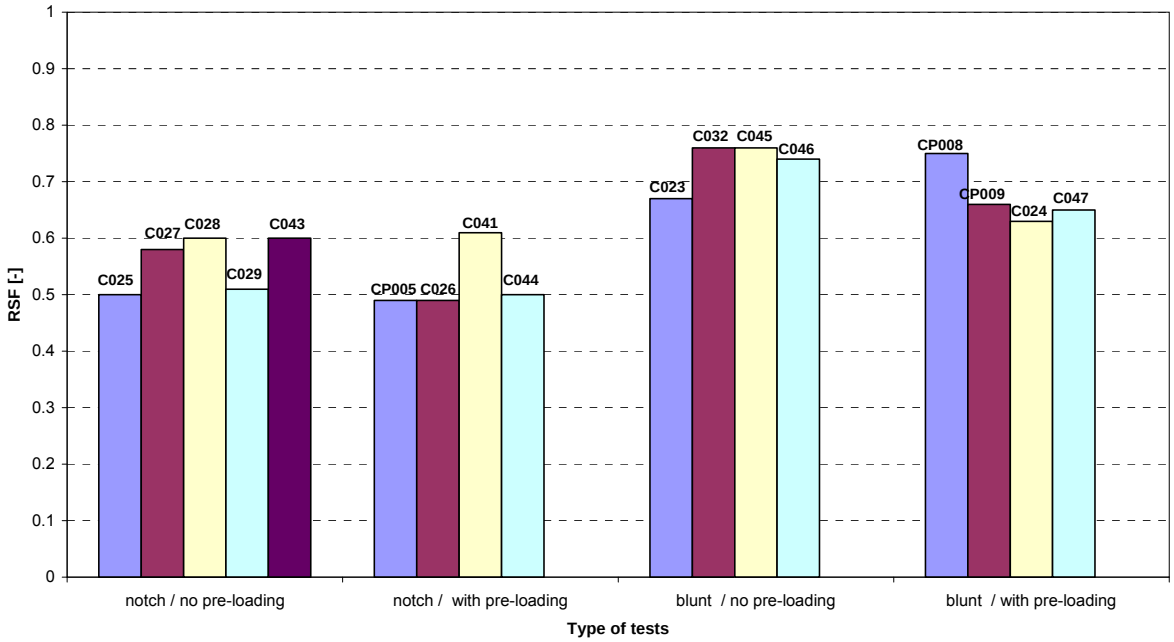

Figure 20: Residual strength factors in tension for 2.1 mm composite plates with zero and 0.25% preload, for notch and blunt impact damage

Composites with compression preload

Table A5 summarises the impact and residual strength tests on the 3.1 mm thick composite plates. In total 26 plates were used in the main composites-compression programme, including 4 baseline plates, 10 plates subjected to impact from 12 mm steel cubes at velocities causing penetration with notch damage, and 12 plates subjected to blunt body impact from 25 mm diameter glass balls causing delamination damage. From the initial baseline compression test it was seen that the composite plates buckle at an approximate load Pb = 38 kN. After discussion with EASA it was decided to apply compression pre-loads to give plates loaded into the post-buckle state (1.4 Pb) and under axial compression in the unbuckled state 0.5 Pb, plus control tests without preload (2kN was applied to stabilise the plates). The compression preload was controlled in the impact tests through the pressure gauge on the hydraulic jack which was previously calibrated so that, for example, a preload of 1.4 Pb requires 53.2 kN which corresponds to 55 bar pressure in the jack.

The impact scenarios were again notch damage from 12 mm steel cube projectiles and blunt impact with delamination damage from 25 mm glass balls. The impact velocities were increased over those used for the composites-tension programme, in order to produce similar damage conditions in the thicker composite plates. For the notch damage tests impact velocities were in the range 126.6 – 136.4 m/s, with impactor kinetic energies in the range 107.4- 124.7 J. For the blunt impact tests velocities were 77.6 – 85.7 m/s, with kinetic energies 58.4 – 70.9 J. When the 1.4 Pb preload was applied the plates always buckled into three cells along the length with a large central buckle. The impact position was always at the centre of the plates, hence always onto the middle point of this central buckle. It was found that the observed impact damage was dependent on whether the projectile impacted the outside of the buckled shell on the *convex* face, or the inside of the buckled shell on the *concave* face. The original planned test programme was extended to study this effect for blunt impact damage, where it appeared to be more significant.

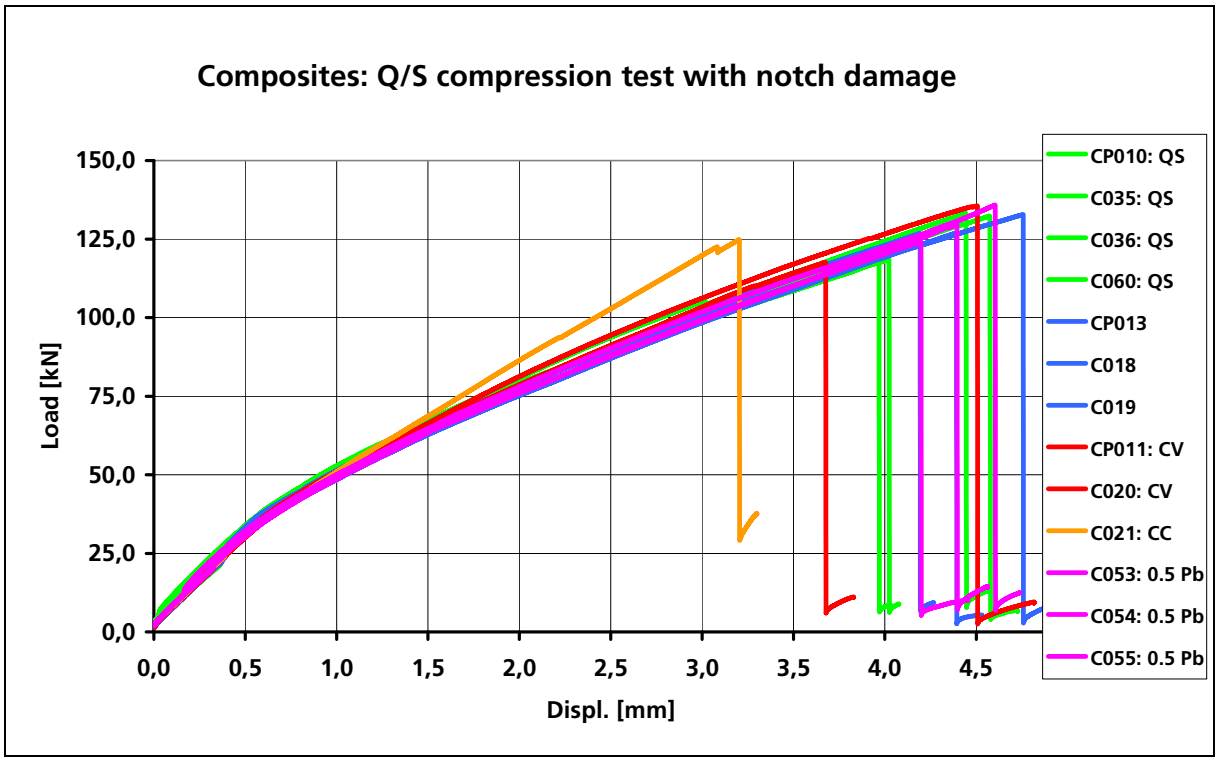

Figure 21: Compression test curves for 3.1 mm composite plates with notch damage
Curve colours: green: baseline (no impact), blue: preload 0, lila: preload 0.5 Pb, red: preload 1.4 Pb (convex), orange: preload 1.4 Pb (concave)

Fig. 21 shows the Q/S compression load-displacement curves for the plates with notch damage, together with the baseline compression test curves. It is seen that all plates, including those with extensive notch damage, had the same initial stiffness properties, and all buckled at about the same point (~0.6 mm displacement, ~ 38 kN). After initial buckling the buckle amplitude increased significantly, as seen by the nonlinearity in the test curves, however, even with notch damage the continued buckling and final collapse load were not significantly reduced by notch damage. Note that in these impact tests with preload the impact point was on the convex face of the buckle in two plates CP011, C020 and concave for C021, which then had a different load curve to failure. It is interesting to note that the curves without preload, ie impacted on a flat plate, and those with 0.5 Pb preload were not significantly different to those impacted in the post-buckled state with preload 1.4Pb. In fact two of the 0.5Pb curves almost coincided with two of the unloaded plates and overlay them in Fig. 21. The RSF values of all plates were in the range 0.89 – 1.02 showing that the notch damage which caused significant visible damage to the plates, see photos and thermography data in Annex B, does not influence the buckling failure strength of the plates, which confirms the unexpected result first seen in the preliminary compression tests with notch damage. Possible explanations for this are discussed at the end of the sub-section. Note that the one notch test C021 with a concave impact, was at a lower velocity of 93.5 m/s which caused rebound plus notch damage. The RSF was 0.94, which was in the range of the unloaded and preloaded convex impact cases. It was decided that a detailed study of notch damage under concave impact was not warranted.

Fig. 22 shows the compression load-displacement curves for the blunt impact tests with glass balls to initiate delamination damage. Included are four baseline curves on undamaged plates (green), three tests with no preload (blue), three tests with 0.5 Pb preload (lila), three tests with 1.4 Pb preload and convex impact (red), and three tests with 1.4 Pb preload and concave impact (orange).

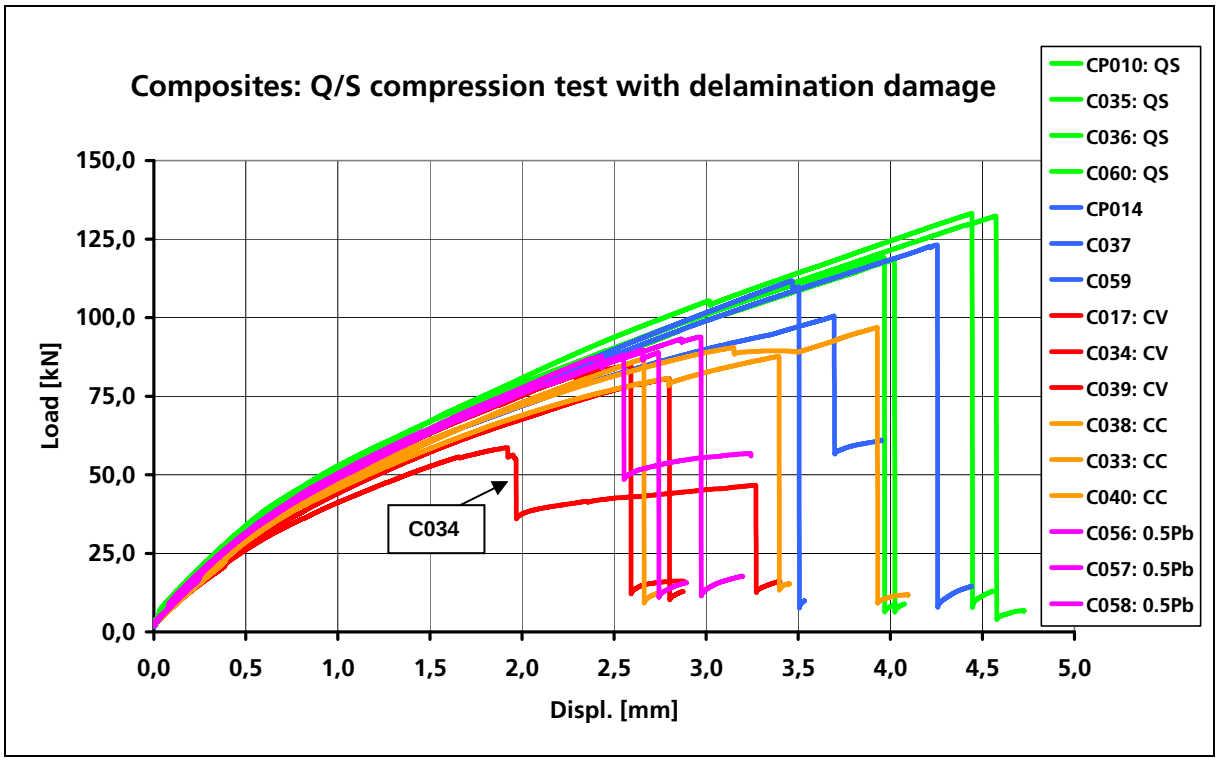

Figure 22: Compression test curves for 3.1 mm composite plates with blunt impact damage Curve colours: green: baseline (no impact), blue: preload 0, lila: preload 0.5 Pb, red: preload 1.4 Pb (convex), orange: preload 1.4 Pb (concave)

In all these blunt impact tests there was little or no visible damage on the front face, with some splitting of the rear 45° plies on the back surface, see Annex B. It was observed that the concave impact tests led to considerably more visible back face damage than the convex impact tests. The thermography images show large delamination regions around the impact position in all plates, with differences apparent between convex and concave impact cases. Fig. 21 clearly shows that these plates fail earlier than those with notch damage with a wider range of RSF values of 0.49 - 0.85 indicating a more significant residual strength reduction and a wider range of behaviour. The test curves show that with delamination damage buckling is initiated at lower loads around 20 kN compared with the baseline tests, and as the damage propagates the failure modes are changed. The departure from the baseline test curves is seen to be most significant for the convex buckle impact tests. Note that in test C034 there was some bending deformation observed between the clamps and the end of the side supports, which led to the drop in the test curve at 1.8 mm and led to the low RSF value. The curves for the three tests with preload 0.5 Pb, which were thus impacted in the unbuckled state are seen to lie between the preload 0 and preload 1.4 Pb curves, and are closer to the buckled plate curves. These tests showed better reproducibility than the tests impacted in the post-buckle state. They show that there is a noticeable reduction in residual strength after blunt impact with compression preloads without buckling.

Fig. 23 provides an overview of the RSF values from compression tests on the 3.1 mm composite plates, with notch and blunt impact damage. It shows clearly the magnitude of the compression plate buckling strength reductions due to notch and blunt impact damage. For notch damage with and without compression preloads, compression strength reductions are less than 10%, indicating that notch impact damage in compression is not a critical design factor in thin plates which fail by buckling. With 0.5 Pb preload there was no significant reduction in RSF compared with unloaded plates. For 1.4 Pb preload there is a small tendency for the strength reduction to be a little higher than for unloaded plates. The effect is very small with mean RSF of 0.97 for plates with 0.5 Pb and zero preload and 0.94 with the preload into the post-buckled state 1.4 Pb. The explanation for the weak interaction between

notch damage and buckling failure load lies probably in the 3-cell buckled shape seen in the tests, as shown schematically in Fig. 24. The notch damage is localised to the impact position at the plate midpoint, in the centre of the mid-plate buckle. It appears that the plate stresses are not high in this region since at the final collapse of the plate, fracture usually occurred away from the midpoint at the line between the 1st and 2nd cell buckles, which was about one third of the distance along the plate. This could explain why the notch damage does not propagate and lead to plate failure, as was the case for the tension tests above where the tensile stresses acted over the full plate width so that damage propagated from the central notch across the plate .

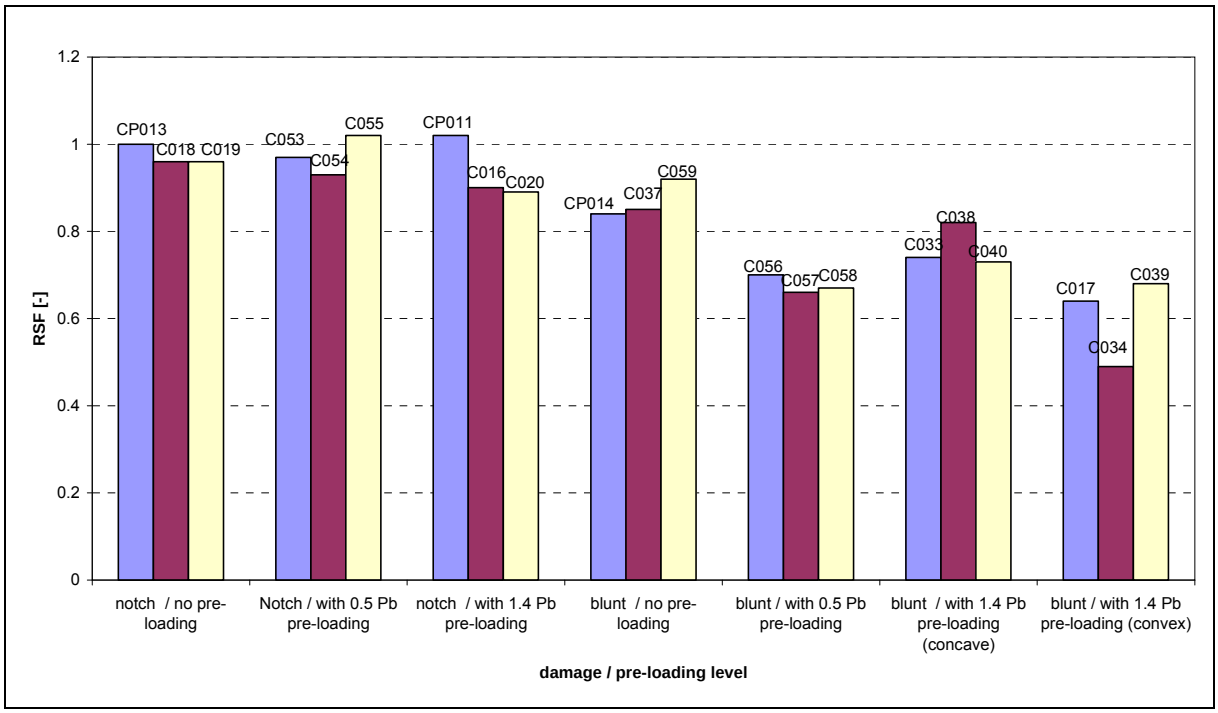

Figure 23: Residual strength factors in compression for 3.1 mm composite plates with zero, 0.5 Pb and 1.4 Pb preload, for notch and blunt impact damage

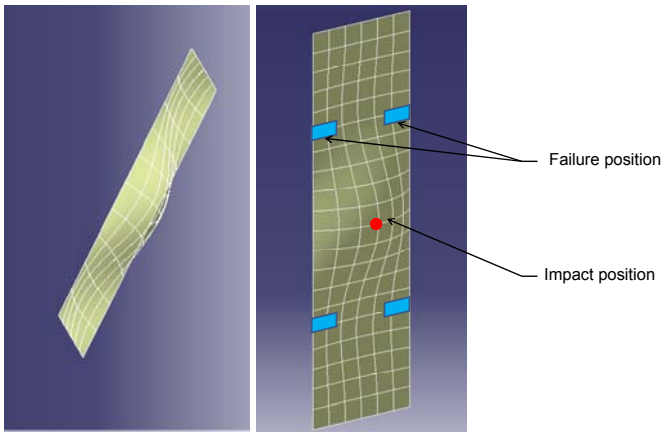

Figure 24: 3-cell buckled shape and failure position of the plate compared to the impact mid-point where delamination occurs

In the case of blunt impact there is a more significant reduction in RSF values, which increases with preload. Without preload RSF = 0.84, and mean values with 1.4 Pb preloads are 0.76 for concave impact and 0.60 for convex impact. For preloads 0.5 Pb in the unbuckled state, mean RSF was 0.68, which is intermediate to the concave and convex buckled plates with 1.4 Pb compression load. What is also noteworthy here is that the strength reductions are higher with convex impact, despite the visible damage after impact

being much greater for the concave impact tests. The reason for this behaviour follows from the thermography data which indicate a larger delamination area at the plate midpoint for the convex impact case, which grows under the bending stresses in the central buckle as the plate is loaded. The larger delamination damage area in the plate finally causes buckling collapse at lower load levels than for the concave impact case, and of course for the notch damaged plates with damage localised at the plate midpoint. The additional tests carried out for compression loaded plates in the unbuckled state with 0.5 Pb do confirm that there is a significant reduction in residual strength with compression preloads and blunt impacts, which is not dependent on the impact taking place in the post-buckled plate.

Aluminium with tension preload

Table A6 summarises the impact and residual strength tests with 2.0 mm thick aluminium plates in tension with measured load-deflection curves shown in Fig. 25. The tensile test procedures were the same as in the composite-tension programme, without preload, and with longitudinal prestrains of 0.25%. All tests were with 12 mm steel cube projectiles with velocities in the range 92.9 – 171.5 m/s, kinetic energies 57.9 – 148.4 J. Most tests were at velocities high enough to cause notch impact damage. Some tests were carried out at lower velocities to cause an indentation with rebound. However, it was not found possible with the sharp edged steel cube to reliably obtain a plastic indentation without impactor penetration or local cracks in the plate. This would be possible with a steel ball projectile, but it was decided that aluminium plate indentation was not so important to justify a test programme with other projectiles.

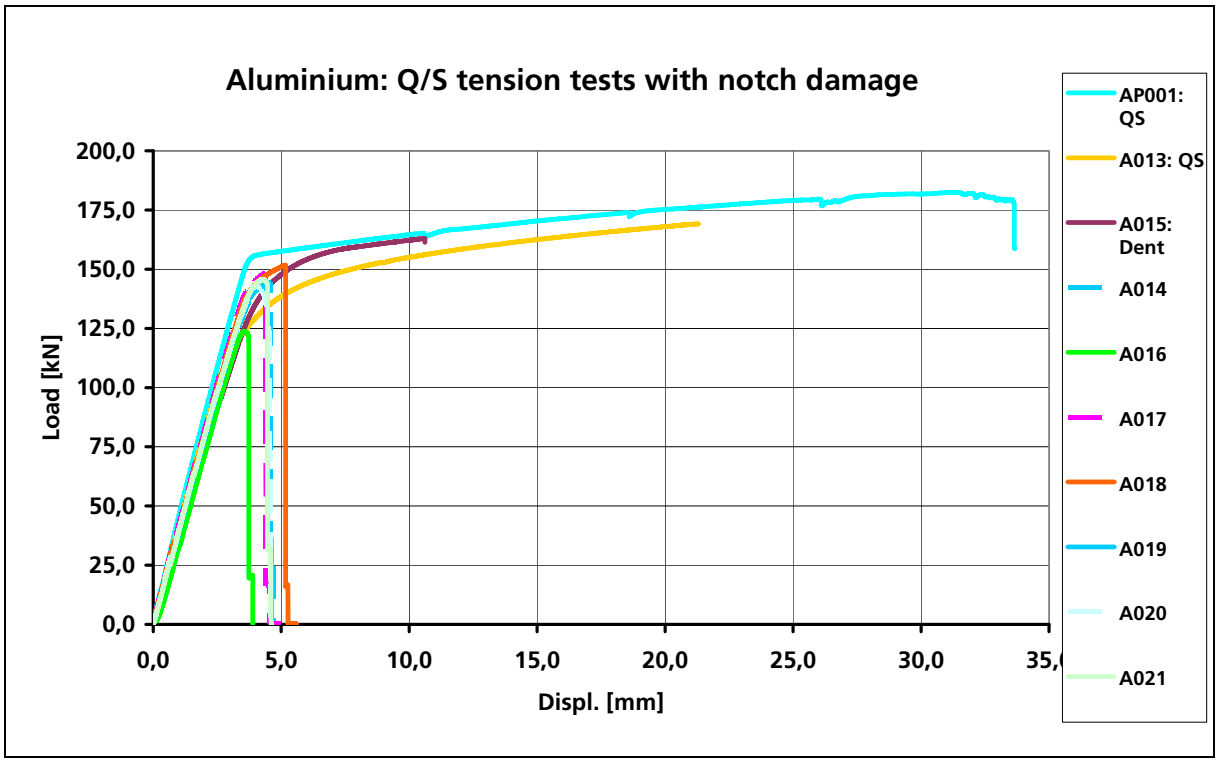

*broken curve indicates no preload

Figure 25: Tensile test curves for 2.0 mm aluminium plates with notch damage

Two baseline strength tests are also included in Fig. 25, which showed an initial elastic response, with onset of yield and steady plastic flow until ultimate failure at extensions of 21.2 mm and 34 mm. In test A015 there was rebound at impact due to the flat contact, which led to a plastic indentation without cracks. In the Q/S test there was plastic flow similar to the undamaged baseline specimens. The test was stopped at 10.8 mm displacement before ultimate failure, due to debonding in the tabs, giving an RSF value of 0.92. This single indentation test served to show that the residual strength with large indentation damage was

not significantly reduced. In the remaining tests there was notch damage with a hole in the plate, or the cube was stopped by the plate but caused notch cracks on contact. In all these remaining Q/S tests 2 main cracks initiated at the notch hole or notch crack and propagated transverse to the plate, leading to brittle failure at about 4 mm extension and loads clearly lower than the baseline plastic failure strengths. This demonstrates a clear notch embrittlement for aluminium plates in tension, with RSF values in the range 0.70 – 0.86. There was no strong effect of tensile preload on residual strength.

Aluminium with compression preload

Table A7 summarises the impact and residual strength tests with 2.0 mm thick aluminium plates in compression, with detailed load-deflection curves shown in Fig. 26. The test procedure again followed that established for the composite compression tests, as discussed for the prescreening tests § 4.2. Compression preloads were zero or in the post-buckling region at 1.5 Pb, based on the measured buckling load of 20 kN for the 2 mm aluminium plates. The impact tests were all with 12 mm steel cube projectiles at velocities in the range 89.6 – 133.9 m/s, kinetic energies 53.8 – 120.1 J. As in the tension tests, impact velocities were reduced in order to obtain some indentation damage, without cracks. However, this was only achieved in plate A010. All other tests led to a large hole damage or the cube was stopped by the plate, but caused cracks at the impact point.

As Fig. 26 shows that all damaged plates (except for AP004) buckled below 20 kN load and on loading the 3-cell buckles increased in amplitude and above about 3 mm displacement a steady plastic flow developed at a constant loads in the range 50 – 55 kN. Buckling collapse or fracture was not reached, even with notch damage, so that all tests were stopped at about 5 mm displacement. Plate AP004 buckled locally near the tabs as explained in the pre-screening test discussion above. The test curves followed the trend of the baseline curves without damage, indicating that despite the plates having holes or cracks up to 25 mm in size at the centre, this has little influence on the buckling failure mode, or collapse loads. The RSF values were in the range 0.95 – 1.01, indicating how unimportant notch damage, with or without preloads is for thin aluminium plates subjected to compression loads with buckling failures.

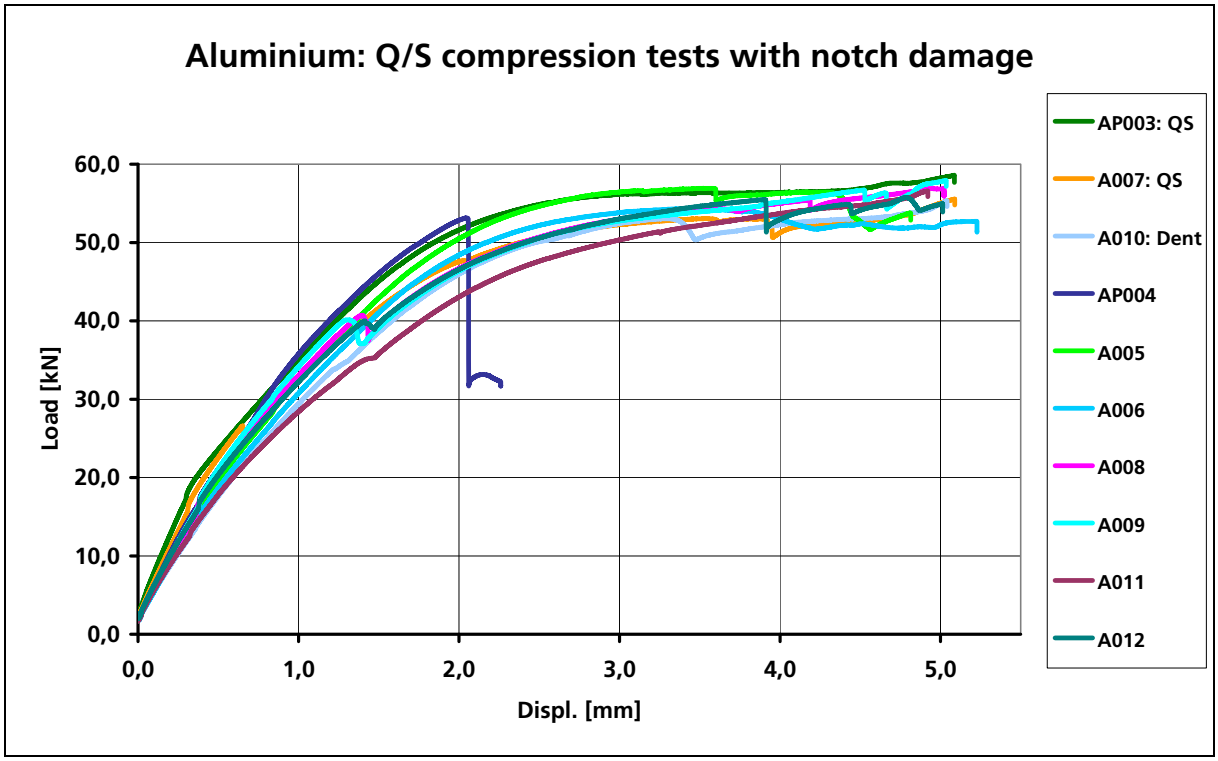

Figure 26: Compression test curves for 2.0 mm aluminium plates with notch damage

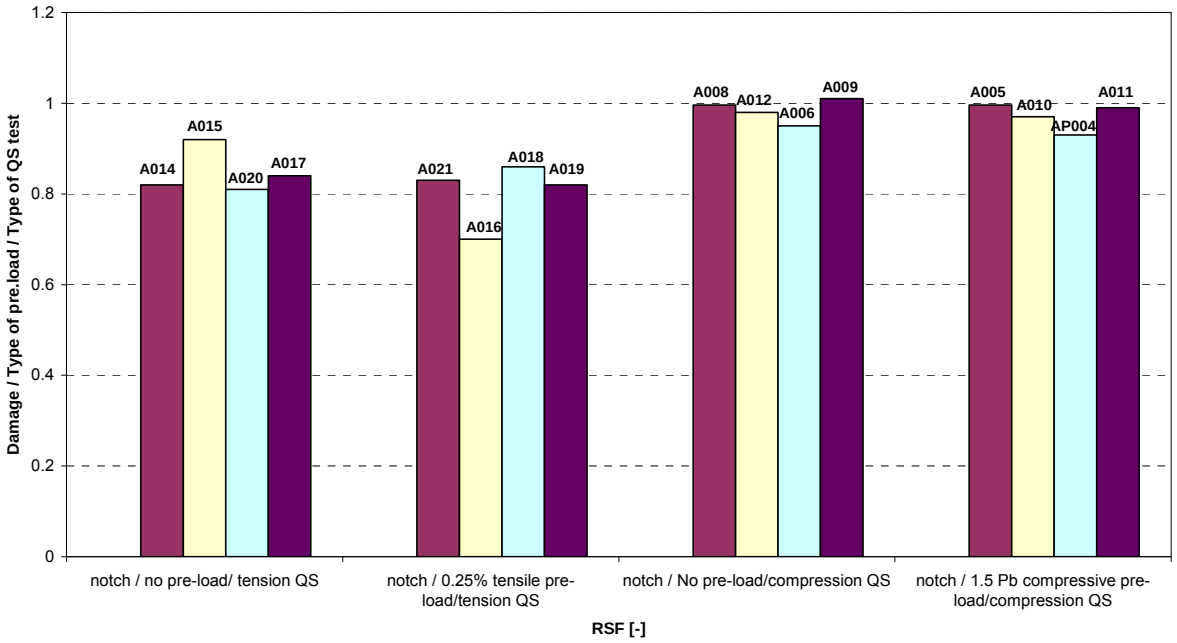

Figure 27: Residual strength factors in tension and compression for 2.0 mm aluminium plates with and without preload, for notch impact damage

Fig. 27 summarises the RSF values for both the tension and compression test programmes on the 2.0 mm aluminium plates. There is a notch damage effect in tension with RSF values in the range 0.70 – 0.86, with no clear trend to indicate that 0.25% tension preloads lead to a reduced residual strength. For compression buckling failure it is again found that despite considerable notch damage in the plates, the RSF values are 0.95 -1.01, which suggests the explanation provided in Fig. 24 for the composite plates also applies here. Again there is no clear effect of buckling preloads on residual strength for aluminium plates.

5.3 Analysis of impact damage and preload

Although LIBCOS is focussing on the influence of preloads on impact damage, it should be emphasised that the test programme itself provides valuable information first on the effect of the impact load case on residual strengths, and second on how this is influenced by quasi-static preloads, if at all. The bar charts in § 5.2 above have given a first overview of the influence of impact damage and preloads on the residual strength of composite and aluminium plates. In some cases the magnitudes of the effects were to be expected, but in other cases not. The data presented were of course based on very specific impact scenarios, plate geometries and materials. Before some general guidelines and recommendations can be drawn from the specific test data presented, it is necessary to have an understanding of the damage mechanisms and their role in determining plate failures and residual strengths. This section discusses the test data presented in § 5.2 and attempts to relate the residual strengths to the observed damage after gas gun impact.

In the case of gas gun impact tests it is almost impossible to reproduce precisely the test conditions. There is a scatter on impact velocity due to the nature of the test which is based on pressure in the gas gun tanks: air pressure, moisture and design of sabots also influence impact velocity. Impact point and impact angle depend on the trajectory. As stated above, with steel cubes the angle of the projectile on contact, which determines if it is face, edge or corner impact can determine the local damage and penetration. A well established parameter for monitoring impact conditions is the impact energy, which can also translate to other impact scenarios than the 12 mm steel cube used here. It is also a parameter used by the aircraft industry to categorise impact scenarios. This parameter is used in this section to analyse the RSF data in more detail, looking for possible anomalies and explanations.

Another important factor is the damage state after impact. For the aluminium plates a convenient impact damage parameter is the notch size across the plate width. For composites internal damage after impact was monitored by thermography and thermography data are shown in detail in Annex B for each composite plate tested. The damage area was measured quantitatively by first marking the damage area on the thermography image with a closed boundary, then using a graphics program to computer this area. The analysis was carried out on all the post-impact composite thermography images, which permits a study of impact damage area on residual strengths.

Composites with tension preload

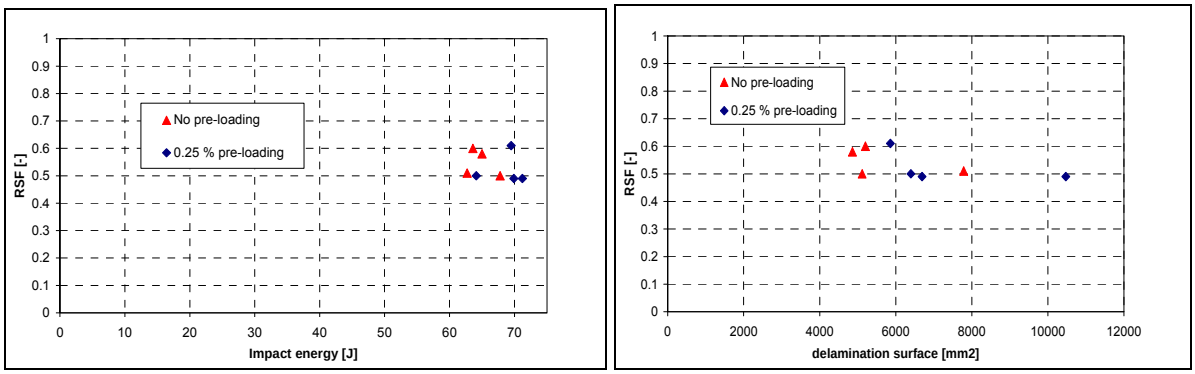

a) **b)**

Figure 28: Composite-tension with notch damage. Influence on RSF of:
a) impact energy and b) damage area

The most significant reduction in RSF from the complete test programme was from notch impact tests on composite plates under tensile loads, as seen in the bar chart Fig. 20. This showed a small additional reduction in RSF when 0.25% prestrains were applied, which could also be interpreted as scatter due to the small number of plates tested. Fig. 28a shows the RSF for the notch tests plotted against the impact energy. It shows that provided the impact energy is high enough for penetration in these notch tests, there is no change in RSF as the energy is increased. There is a tendency for a slightly lower RSF with 0.25% tensile preloads, which does not appear to be influenced by impact energy. Fig. 28b considers the influence of impact damage, by plotting RSF against measured damage area in mm². Fig. 28b shows that damage area is in the range 5000 – 10 500 mm², for this test programme. It appears that the damage area may be significantly larger for notch impact with tensile preload. However, this seems to have no influence on the measured RSF values. It is concluded that for severe notch damage, the size of the notch (which due to the 12 mm steel cube is fairly constant) determines the strength reductions, and additional delamination damage is of secondary importance.

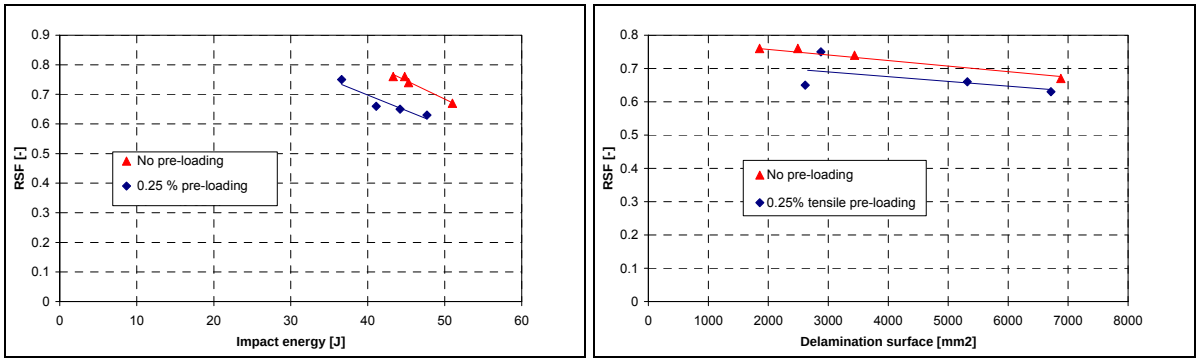

a) **b)**

Figure 29: Composite-tension with blunt impact. Influence on RSF of:
impact energy and b) damage area

Fig. 29a shows a similar analysis applied to the blunt impact tests. Here it is seen that the differences in impact kinetic energy do have an influence on the RSF value, with higher energies causing a reduced RSF. Fig. 29b also shows some correlation between RSF and delamination area. For these blunt impacts delamination area is in the range 2000 – 7000 mm², but with reduced RSF for larger delamination areas. The graphs reinforce the previous conclusion that for blunt impacts there is a small but measurable reduction in RSF of about 10%, which may be explained if the tensile preload causes greater delamination in blunt impact.

Composites with compression preload

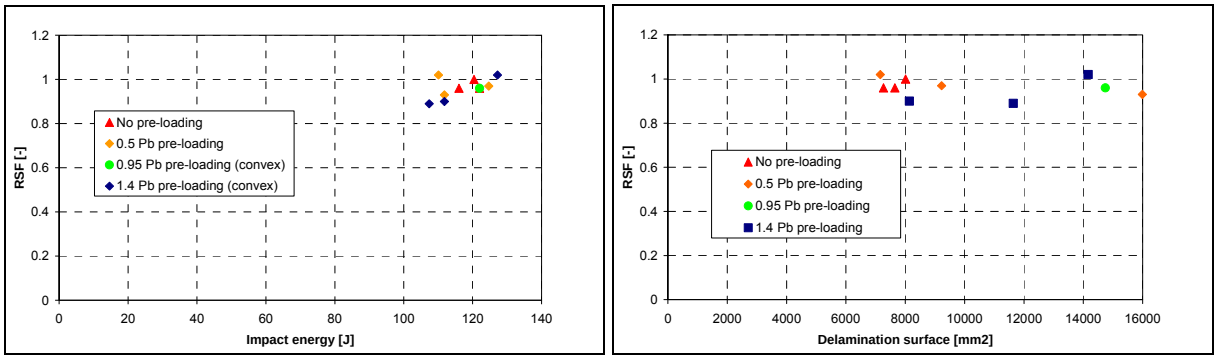

a) **b)**

Figure 30: Composite-compression with notch damage. Influence on RSF of:
a) impact energy and b) damage area

In the case of compression preloads in the pre-and post-buckled region the RSF values are little influenced by notch damage and it even appears from Fig. 30a that increasing impact energy leads to higher RSF values closer to unity. The RSF values for the pre-buckled plates 0.5 Pb are very close to and sandwiched by the zero preload and buckled preload 1.4 Pb data. Fig. 30b indicates large damage areas from 7000 – 15 000 mm². Generally the preloaded plates have considerably greater damage area than the unloaded plates, but this damage in the plate does not have a strong influence on residual strengths. This may be explained if the notch and delamination damage is in the plate central impact zone, but due to the complex buckling stress field, higher stresses leading to failure are away from the centre.

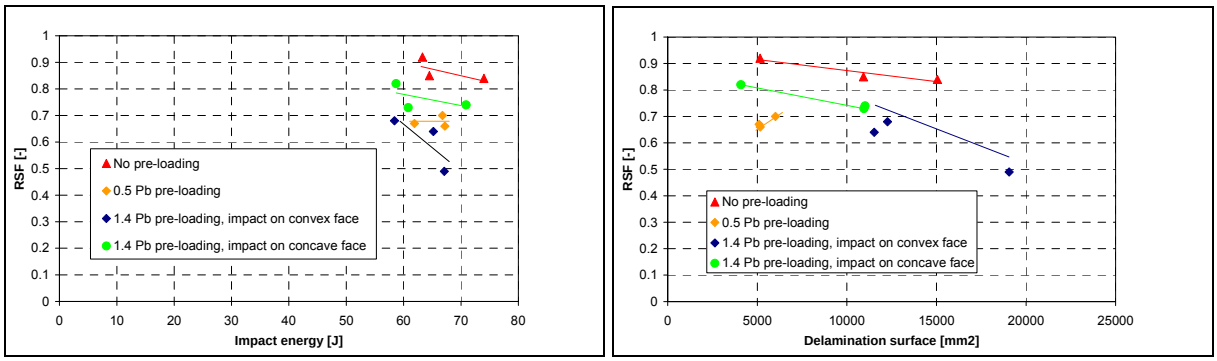

a) **b)**

Figure 31: Composite-compression with blunt impact. Influence on RSF of:
a) impact energy and b) damage area

In the case of blunt impact on composite plates in compression, Fig. 31a shows good correlation between lower RSF values and higher impact energies, particularly for convex buckling cases. There is a clear tendency of lower RSF for compression preload, with smallest reduction for 1.4 Pb preloads and concave impact, and largest for the case of convex impact. The pre-buckled plates with 0.5 Pb are sandwiched between these two

extremes. The significant differences between convex and concave impacts are clearly shown in the measured damage areas in Fig. 31b. The smallest damage areas are seen in the concave impact cases from 4000 – 11 000 mm², with the largest damage areas 11 000 – 18 000 mm² in the convex impact plates. The plates without preload had 5 000 – 15 000 mm² damage and the pre-buckled plates with 0.5 Pb preload showed the smallest damage area 5 000 – 6 500 mm². Note that the visible damage in the concave impact plates after impact was considerably higher than in the convex impact plates, which thermography shows had more internal delamination damage. This high damage area causes failure at lower loads and hence lower RSF values, than in the concave plates and those without preloads.

Aluminium with tensile preload

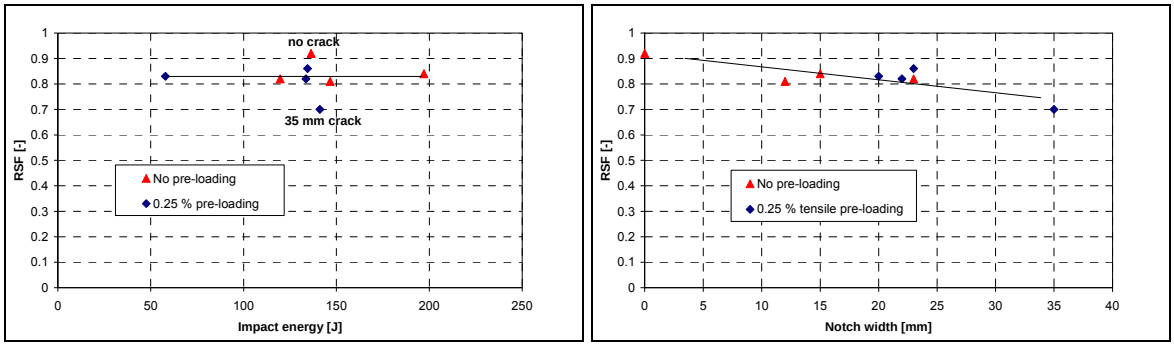

a) **b)**

Figure 32: Aluminium-tension with notch damage. Influence on RSF of:
a) impact energy and b) notch size

Fig. 32a plots the RSF parameter against impact energy for the 12 mm steel cube impacts on 2 mm aluminium plates with and without 0.25% tension prestrains. The expected reduction in RSF from the notch effect is seen, but the RSF values in the range 0.70 – 0.86 are much higher than those for the composite plates. From Fig. 32a there is no apparent influence of impact energy on strength reduction for notch damage. It follows that the energy should be high enough to cause cracks or penetration, but higher energy impacts do not appear to influence the residual strength. Fig. 32b considers the effect of notch size on RSF, in this case the size of the crack or hole across the plate width direction was measured from the impact damaged plates. It also indicates a clear influence of notch size in reducing the RSF. The datapoint with zero notch size in the figure is plate A015, which was dented on impact without cracking. There is a small effect of larger notch size for the tests with preload compared to unloaded plates. During the gas gun tests on the aluminium plates it was observed that the cube passed more cleanly through the plates with tensile prestrains leaving a hole. For unloaded plates there were more bending vibrations on contact, with plastic indentation and less cracking. Thus it appears that tension preloads may change the local damage at contact, but this has a secondary effect on residual strength as long as the impact energy was high enough to cause a notch.

Aluminium with compression preload

A similar analysis is carried out here for the influence of impact energy and notch size on aluminium plates under compression buckling loads. Fig. 33a shows first that notch damage has only a small influence on RSF in compression, with values 0.95 – 1.01. Further, the residual strengths are not influenced significantly by impact energy. Again Fig. 33b shows a tendency for the prebuckled plates to have a higher notch size, which is accompanied by a small reduction in RSF. However, it is again apparent that significant notch damage in the plate centre plays a minor role in the plate collapse in buckling, since the buckles were observed to increase in amplitude with plastic deformation at higher loads despite the notch damage in the central buckle.

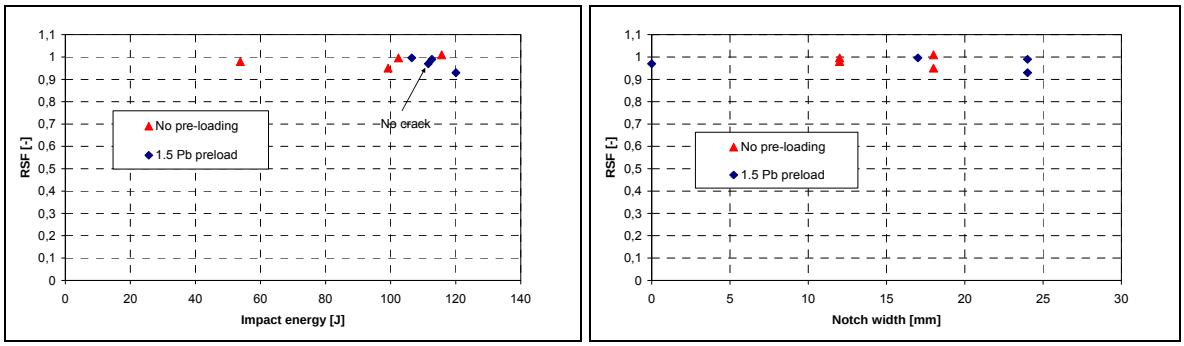

a) **b)**

Figure 33: Aluminium-compression with notch damage. Influence on RSF of:
a) impact energy and b) notch size

6 Significance of results for DT compliance

LIBCOS is concerned with assessment of impact damage in composite panel structures in order to improve guidelines for the damage tolerance (DT) of composite aircraft structures under impact loads. Sierakowski and Newaz [21] give the definition: 'damage tolerance for aerospace composites is defined as the capability of the composite structure to sustain an impact event (with barely visible impact damage) and retain appropriate residual strength'.
Based on this definition the procedure to assess DT consists of the steps:

1. Damage initiation through suitable impact tests, using real or idealised conditions for a relevant impact scenario.
2. Damage inspection, evaluating its nature and topology.
3. The measurement of residual strength, when the structure is stressed under simulated real conditions.
4. Compare residual strengths with aircraft design loads (DLL, DUL) for the structure.
5. Evaluate results with DT criteria for aircraft structures (impact damage categories, BVID, VID, …)

The aim of the present study was to evaluate the influence of quasi-static preloads on the impact damage and residual strength of carbon/epoxy and aluminium panels. This generally requires a great number of tests. Study of the real structures is impossible because of the excessive cost involved. Hence typical test specimens are based on these structures. In this case, flat panel specimens were selected which represent fuselage bay panels between frames and stringers and impact test cases were selected to represent particular damage states or impact scenarios. These may be considered as Level 2 structural details in the test pyramid (Fig. 1). Steps 1 – 3 above have been carried out on the chosen composite panels and impact load cases, with the measured residual strengths presented in detail in §4 and §5 above. Steps 4 and 5 are now considered here in §6 by comparing residual strengths with representative design loads for aircraft panels and considering current DT criteria for aircraft structures under impact. The focus here is on the influence of preload on impact damage and residual strengths. In order to give an assessment of the influence of preload on DT of composite panels, reference is made to other test programmes reported in the literature. In order to compare different test programmes it is necessary to consider the important test parameters which influence residual strengths and DT. These are briefly discussed here.

Test programmes are concerned with measuring residual strengths in tension or compression in composite plate specimens with impact damage arising from drop weight low velocity impact tests (LVI) or gas gun high velocity impact tests (HVI). Most studies carried out do not consider the influence of preloads. Typical results for CFRP materials under impact are reviewed in [21], [22], whilst basic failure mechanisms under impact and their influence on residual strengths are also discussed in [23] - [25]. The behaviour from studies on small impacted test specimens under tension and in compression after impact (CAI) has a generic form, shown schematically in Fig. 34. This shows how the residual strength is critically dependant on the impact damage, which is characterised most simply by the impact energy. In the figure E_D is the energy at onset of delamination, E_F at onset of fibre fracture or penetration. For impact energies $E < E_D$ the plate behaves elastically, there is no significant impact damage, the impactor rebounds and the residual strength is close to that in a plate without impact. For $E > E_D$ the impactor will also rebound but the plate has delamination damage, which increases with impact energy, and can lead to a significant reduction in residual tensile strengths and CAI strengths. However, for hard body impacts there will be a higher impact energy E_F at which significant fibre fracture takes place at impact, or even penetration of the plate. In the quasi-static tensile or CAI test the plate now behaves as a plate with a hole, which can lead to a low residual strength. However, for impact energies $E > E_F$ the projectile passes through the plate and there is no growth of impact damage. As a result for higher impact energies the residual strength tends to remain constant. The critical energies E_D and E_F depend on many factors, plate material, plate size, thickness and layup, impactor size, mass and velocity, plate boundary conditions, etc. If design limit load DLL and

design ultimate load DUL are known for the panel (DUL = 1.5 DLL in FAR 25 [2]) under the relevant load condition, then the residual strength curve Fig. 34 may be used to define an allowable damage limit ADL, when residual strength falls to DUL, and a critical damage threshold CDT, when residual strength falls to DLL.

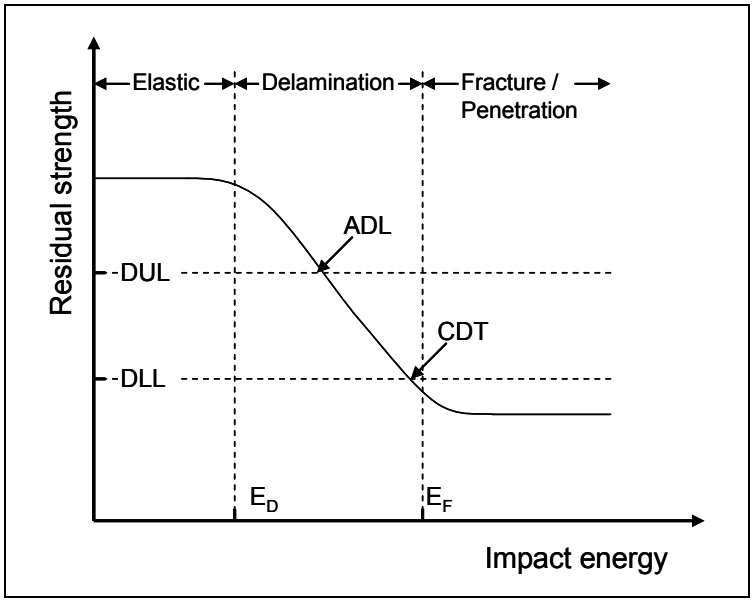

Figure 34: Schematic of residual strength in plates as function of impact energy with zero preload
Critical impact energies: E_D – onset of delamination, E_F – onset of fracture,
DUL – design ultimate load, DLL – design limit load,
ADL – allowable damage limit, CDT – critical damage threshold

The key parameter in the tests is thus E/E_D, together with E_F. When tensile preloads are applied a second important parameter is P/P_F the ratio of preload to ultimate failure load in an undamaged plate, or alternatively $\varepsilon/\varepsilon_F$ the applied tensile prestrain to the laminate tensile failure strain. Because the strain field in tension is uniform these two parameters will have similar values. The interest now is how P/P_F changes the residual strength curve Fig. 34 with zero preload. In particular will it lower the curve so that ADL and CDT are reduced?

However **i**n assessing the nature of impact damage, compressive preloads, and the coupling between the two, there are three characteristic non-dimensional parameters, as discussed in [8]. This is because in the residual strength tests, ultimate failure may be due to a buckling failure, or a composite materials fracture depending on the specimen geometry and load conditions. The parameters are now the critical damage energy E/E_D, the preload/buckle load P/Pb which can affect the dynamic response and impact damage when this ratio is ~1 (at a state of neutral equilibrium), and for composite laminate failures $\varepsilon/\varepsilon_F$ which may be compression strain but could be bending strain or shear strain if ultimate failure is in the post-buckle region.

6.1 Composites with tension preload

To provide an assessment of the damage tolerance of the 2.1 mm composites plates under tensile loads, all the residual strength data from both blunt and notch impacts with and without tensile preloads is plotted on a single graph in the format of Fig. 34. The result is Fig. 35, on which representative values for DLL and DUL are marked. As discussed in §4.1 typical values for these composite fuselage bay panels are DLL = 0.25% strain, DUL = 0.4% strain. Based on the DLR impact tests it is estimated that the critical impact energy at

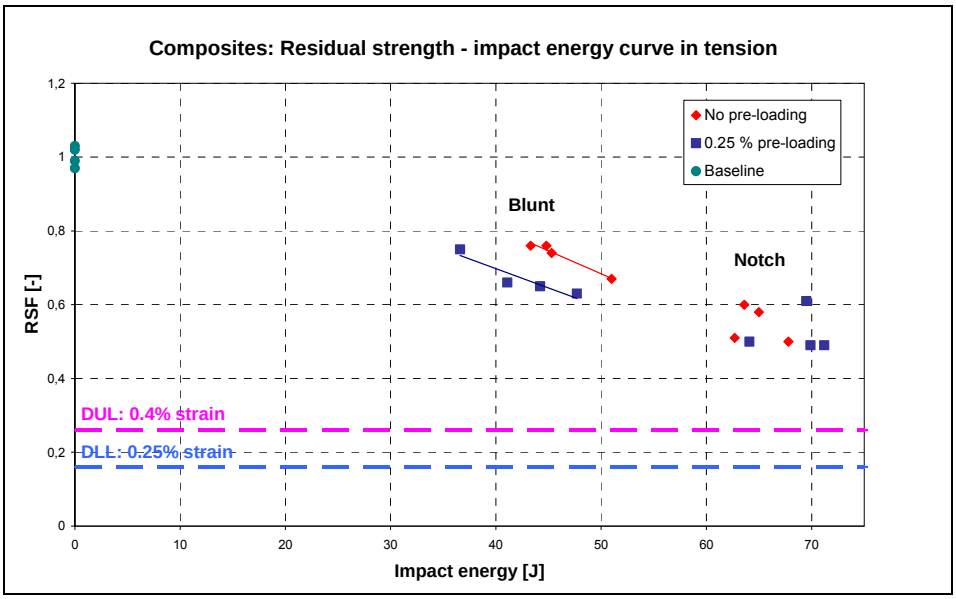

Figure 35: Residual tensile strength – impact energy curve for 2.1 mm composites (Preload: $P/P_F = 0.16$, $\varepsilon/\varepsilon_F = 0.17$, Critical energy estimates $E_D \sim 20$ J, $E_F \sim 55$ J)

fracture for the panels from these small projectiles is $E_F \sim 55$ J, and from literature data and other DLR tests a value $E_D \sim 20$ J is expected. With this information it is seen that the tensile data fit very well into the schema of Fig. 34 for assessment of damage tolerance. The blunt impact data are at energy levels intermediate to E_D and E_F, where they fall noticeably with small increases in impact energy. For the notch impact tests with energies above 60 J there is penetration and the residual strength is constant with RSF = 0.5. It would be expected that for these steel cube projectiles residual strengths would remain at this value at higher impact velocities, since DLR experience shows that at higher velocities there is a cleaner exit hole with less delamination. The effect of tensile preloads at the level $P/P_F = 0.16$ is to lower the damage tolerance curve without preloads a little, reducing the residual strengths by about 10%. On this non-dimensional scale DUL = 0.26, showing there is a significant safety margin in tension for the composite panels under small object FOD impacts with maximum preloads equal to DLL.

The DLR results with tension preloads are compared now with related data in the literature. It should be noted that no equivalent test programme with gas gun impacts on larger composite panels of size 500 mm x 200 mm followed by residual strength tests has been found. However much of the reported work is consistent with the schematic DT curve Fig. 34, which aids the discussion. Brief information about the test conditions and load cases from the other studies is summarised below for readers who are interested. In all cases test plates were much smaller than DLR specimens and are generally Level 1 coupons, with preloads usually much higher than the maximum value $P/P_F = 0.16$ in the DLR tests. In [26] tensile preloads were $P/P_F = 0.30$, which led to lower RSF values for blunt impacts and a 20% reduction due to preload, which is consistent with DLR data. High tensile preloads in the range $P/P_F = 0.2 – 0.75$ were applied in [27], [28] in order to determine a failure threshold curve for composite laminates subjected to combined tensile preload and gas gun impacts. Strong interactions were found, such that for $P/P_F > 0.6$ critical impact energies could be reduced to 12% of those measured with $P/P_F = 0.3$. This would cause large changes to the DT curve such as Fig. 35 for high P/P_F values. These coupon test results are scientifically interesting, but load conditions are well outside the range applied for aircraft DT studies and applied in the DLR work. Biaxial prestress conditions with impact were studied in [10] and [29], but without residual strength tests. Conclusions from the low velocity drop weight impact tests in [10] with biaxial tension prestrains of 0.1 % strain, and shear prestrains of 0.15 %, were that impact damage mode and damage energy absorbed are generally unaffected by these low preload conditions, relevant to aircraft structures. Biaxial tensile prestresses at higher preloads $P/P_F = 0.31$ were applied in [29] to ballistic impact tests on GRP plates and

shown to increase the ballistic limit by 11%. Thus the plate penetration energy at high velocities is increased by biaxial pre-stress, which improves damage tolerance in this case. Thus the limited information available suggests that biaxial pre-stress with impact may not be an important case for further experimental studies.

6.2 Composites with compression preload

To provide an assessment of the damage tolerance of the 3.1 mm composites plates under compression loads, the residual strength data from both blunt and notch impacts with and without compression preloads is plotted on a single graph in Fig. 36. The data point from specimen C034 is excluded here because of a problem with the rails leading to a premature failure (see Fig. 22). For compression preloads in the postbuckling region, a distinction is made between impact on the convex or concave face of the large central buckle. Representative values for DLL and DUL are marked on the figure. These are of course dependent on the structure under consideration, load conditions and selected design criteria. The values chosen here follow the discussion on compression preloads in §4.1 relevant to a fuselage bay panel, which may buckle at DLL, due to the panel size and low thickness. In terms of a measured buckling load Pb, DLL was nominally chosen here to be 1.4 Pb for the 3.1 mm thick composite panels, hence DUL = 2.1 Pb. Based on the DLR impact tests it is estimated that the critical impact energy for fracture and penetration of these 3.1 mm composite panels from these small projectiles is E_F ~ 90 J, and from literature data and other DLR tests a value E_D ~ 30 J might be expected. In these tests the maximum preload was 1.4 Pb = 53.2 kN and, since the mean baseline residual compression strength at buckling failure was 125.9 kN, it follows that the preload factor P/P_F = 0.42. This is much higher than the value 0.16 applied in the tensile preload tests.

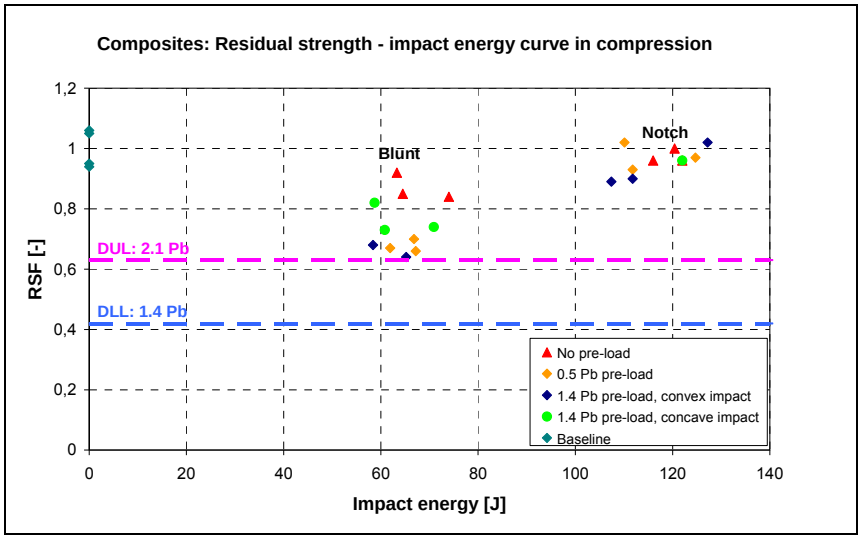

Figure 36: Residual compression strength – impact energy curve for 3.1 mm composites (Preload: P/P_F = 0.42, Critical energy estimates E_D ~ 30 J, E_F ~ 90 J)

Reference to Fig. 36 shows that the compression test data do not fit exactly into the schema of Fig. 34 for assessment of damage tolerance. The blunt impact data are at energy levels intermediate to E_D and E_F and it is seen that RSF falls and is in the range 0.62 – 0.9 (when plate C034 is excluded). Note that the scatter in RSF values for blunt impact is influenced a little by impact energy, but more strongly dependent on the buckled state at impact. For the concave impacts the plate central impact position is in tension, hence constrained so that there is less plate deformation on impact causing more localised damage with less delamination. The situation is reversed in the non-loaded plate and those with P/Pb = 0.5 or 1.4 in the convex case. The plate is closer to neutral equilibrium, hence on impact there are large bending deformations which cause delamination damage over a larger area. Then in the Q/S compression tests into the post-buckle region, leading to buckling failure, the

reduced bending properties over a larger area with delamination growth on loading cause significant reductions in compression strength. The observed behaviour fits into the schema of Fig. 34 in the energy range E_D to E_F, showing significant reductions in residual strength for impacts without penetration.

For the notch impact tests with energies above 100 J there is penetration and the residual strength is in the range 0.9 – 1.1, hence reduced very little compared with baseline plate buckling strengths and the blunt impact residual strength values. In this case there is a tendency for RSF to increase to a value close to 1 as impact energy is increased, probably due to a cleaner exit hole with less delamination damage at higher velocities. Thus it appears that notch damage with compression preloads with high preload ratios $P/P_F = 0.42$ have no significant influence on residual compression buckling strength of the panels. In the context of Fig. 34, it means that residual strengths increase for higher impact energies above E_F ~ 90 J then remain fairly constant close to 1, instead of falling to a constant low value of about 0.5 as seen in the tension preload case.

The consequence for DT is shown in Fig. 36 where the blunt impact RSF data with compression preloads are lower than the unloaded values and are actually reduced to DUL. Since these blunt impacts may be in the BVID category they have reached the allowable damage limit ADL where the RSF must not be below DUL. This appears therefore to be a critical load case for damage tolerance. With larger blunt impactors there could be increased delamination damage with compression preloads, which could lower RSF further. By contrast the notch damage RSF data are close to 1, and well above DUL even for this high preload ratio of $P/P_F = 0.42$, indicating excellent DT under small object FOD.

The major differences in the tension and compression preload results are due to the fact that there is an additional critical preload parameter in the test. As discussed above P/P_F determines the magnitude of the preload compared with the undamaged residual strength, but in addition P/Pb determines the prestress state in the plate when impact takes place. For $P/Pb < 1$ there should be a fairly uniform compression stress, but for $P/Pb \sim 1$ and $P/Pb > 1$ the plate is in a buckled state with bending stresses, which are non-uniform over the plate surface depending on buckling mode. Thus impact damage is influenced by the non-uniform stress field in the plate at impact. In the DLR tests, due to the plate geometry and boundary conditions chosen, the plates buckled into 3 cells and were impacted always at the mid-point. Furthermore, the same buckled shape was usually seen in the Q/S tests up to final fracture. However, fracture in the composite laminates at buckling failure was always by composite fracture in compression or shear/compression at positions about one third along the plate, in the intermediate region between 2 of the 3 buckled cells, not in the central impact zone, as shown in Fig. 24. This explains why in the notch damaged plates with central hole, there was not a significant reduction in residual strength. This was seen in the blunt impact plates, because of the much larger size of the delamination damage regions. Based on this discussion it is apparent that the buckling mode influences residual compression strength and also the nature of the impact damage. The question therefore arises what happens for different plate geometries with alternative buckling modes? In particular, if there is a 2- cell buckle would a central impact cause more damage and lower residual compression strengths further, since the damaged region now coincides with higher laminate stresses at the cell buckle interface? This may require further study by a similar test programme on plates with a lower aspect ratio than those used here. This could not be investigated in this study due to budget and time constraints.

The DLR results with compression preloads are compared now with related data in the literature, in order to gain insight into the significance of compression preloads and buckling on DT. It should be noted that no equivalent compression test programme with gas gun impacts on larger composite panels of size 500 mm x 200 mm followed by residual strength tests has been found. Brief information about the test conditions and load cases from the other studies is summarised below for readers who are interested. In all cases test plates

were smaller than DLR specimens and are generally Level 1 coupons with residual strength tests frequently carried out in a Boeing type compression after impact (CAI) fixture with anti-buckling guides. Preloads are in the range of the DLR tests and often higher, but without buckling due to the test fixtures. The only tests with notch damage were the ballistic impact tests at 922 m/s reported in [30]. These very high energy impacts combined with compression preloads up to 0.7% strain, led to RSF values in the range 0.78 – 1.0 which are consistent with DLR data for the notch damage from steel cubes and indicate that notch damage with complete penetration from small projectiles does not lower damage tolerance in compression at the preload levels in aircraft structures.

The remaining studies were all concerned with blunt impacts causing delamination damage, with constrained compression preloads or with buckling. Preloads into the postbuckling region on 200 mm x 200 x 4 mm plates were considered in [8], where at failure there was a 2-cell buckle. At 32 J impact RSF was reduced to 0.52, which is lower than the DLR values and below DUL on Fig. 36, for preloads P/Pb = 1, but due to the smaller, thicker plate compression pre-strains were 0.32%. It was considered here that the combination of high compression prestrains at the 2-cell buckle interface at the plate mid-point leads to increased damage after impact at the plate centre. Similar effects were observed by Starnes [31] on thick plates with dimensions 248 mm x 114 mm x 7 mm tested in a CAI fixture. With preloads $P/P_F = 0.33$, the RSF value was reduced to 0.35 for 15 J impacts in a gas gun with a φ12.7 mm aluminium ball projectile. Here there was no buckling due to the compression preload, but in the residual strength test there was a 2-cell buckle at ultimate failure. Hence the combination of compression and bending stresses at the plate centre with delamination damage which cause the low residual strengths. Morlo [32] applied high compression preloads up to $P/P_F = 0.5$ on small plates 90 mm x 90 mm x 3 mm in a CAI fixture. At 13.2 J impact an RSF value as low as 0.11 was measured, which indicates a strong interaction between direct compression preloads, without buckling, and impact. However the tests are not representative of aircraft panels due to the very small specimen size and the very high preload $P/P_F = 0.5$. Nettles [33] carried out tests on similar plates 100 mm x 76 mm x 2 mm in a CAI fixture, and obtained smaller reductions in RSF, down to 0.75 for 16 J impact with preloads $P/P_F = 0.57$. These are similar to the DLR values for blunt impact and considerably higher than the RSF data from Morlo [32] although the plates are similar in size. The reason may be that a toughened epoxy resin was used in [33], which reduces impact damage. It could also be due to the thin 2 mm plates, which may fail by buckling in the residual strength test rather than by compression strength failure, giving lower failure loads.

6.3 Aluminium with tensile preload

The damage tolerance of the 2 mm aluminium plates under tensile loads is summarised in Fig. 37, where the residual strength data from notch impacts with and without tensile preloads is plotted on a single graph in the format of Fig. 34. Representative values for DLL and DUL are marked for thin aluminium fuselage bay panels, with the assumption of DLL = 0.25% strain, DUL = 0.4% strain. Based on the DLR impact tests it is estimated that the critical impact energy at fracture for the panels from these small projectiles is $E_F \sim 55$ J. The DLR baseline tests give a maximum preload factor of $P/P_F = 0.42$, much higher than in the composite tension tests. The figure shows that for aluminium the RSF values are in the range 0.7 - 0.9, which are much higher than those from notch impact tests on composite panels. There is no clear tendency for reduced RSF values at 0.25% tensile prestrain, nor does the impact energy have a strong influence provided it is high enough to cause complete penetration by the impactor. This follows because the residual strengths of the notch damaged aluminium plate depend on the notch size in relation to the plate width. All the residual strength values are above DUL, with some strength in reserve, showing there is an adequate safety margin in tension for the aluminium panels under small object FOD impacts with maximum preloads equal to DLL.

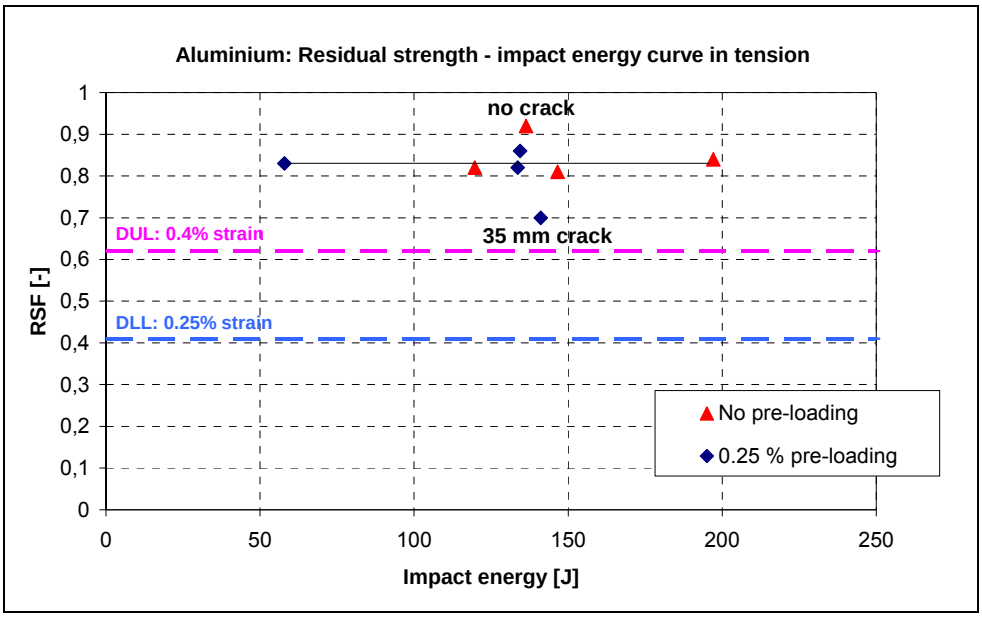

Figure 37: Residual tensile strength – impact energy curve for 2 mm aluminium (Preload: $P/P_F = 0.41$, Critical energy estimates $E_F \sim 55$ J)

6.4 Aluminium with compression preload

To provide an assessment of the damage tolerance of the 2 mm aluminium plates under compression loads, the residual strength data from notch and indentation impacts with and without compression preloads is plotted in Fig. 38. Representative values for DLL and DUL are marked on the figure. In terms of a measured buckling load Pb, DLL was nominally chosen here to be 1.5 Pb for the 2 mm thick aluminium panels, hence DUL = 2.25 Pb. Based on the DLR impact tests it is estimated that the critical impact energy for fracture and penetration of these 2 mm aluminium panels from these small projectiles is $E_F \sim 55$ J. In these tests the maximum preload was 1.5 Pb = 30 kN and, since the mean baseline residual compression strength at buckling failure was 57.1 kN, it follows that the preload factor $P/P_F = 0.52$, which is a high factor. Measured RSF values are in the range 0.9 – 1.0, showing no significant reductions in compression strengths due to notch damage and the buckled preload. The panels had significant reserve strength above DUL for these small object FOD impacts. Higher impact energies with these projectiles would not be expected to reduce residual strengths any further. The explanation for the high residual strengths is that buckling failure was again in the 3-cell mode with large plastic deformations near the plate supports and at the interface between the buckled cells, which was not strongly influenced by the central holes in the panel produced by the cube impacts.

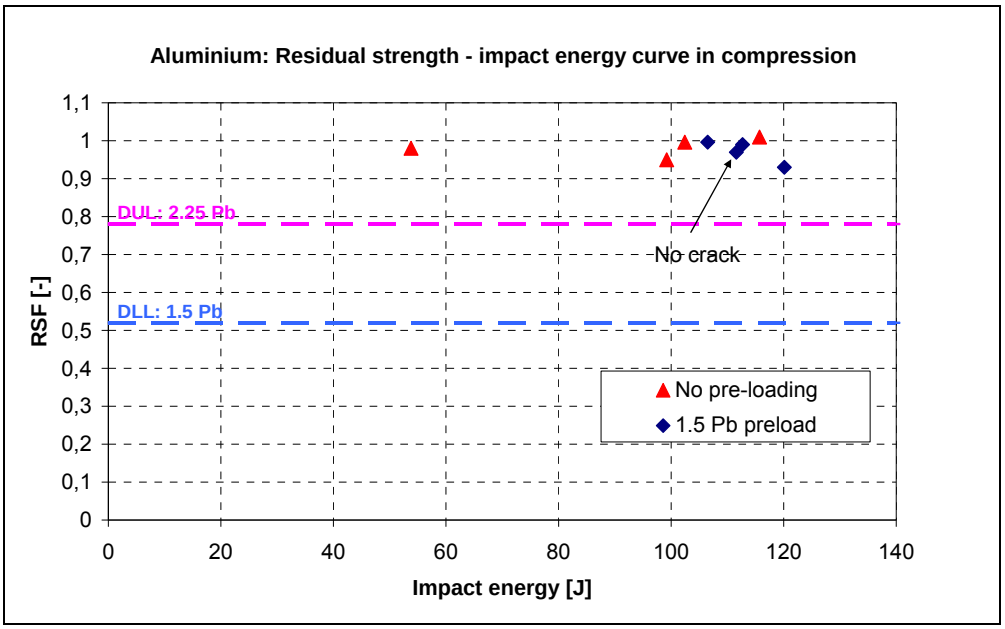

Figure 38: Residual compression strength – impact energy curve for 2.0 mm aluminium (Preload: $P/P_F = 0.52$, Critical energy estimates $E_F \sim 55$ J)

7 Conclusion

A test programme investigating the influence of pre-loads on the residual strength of composite panels after impact, representative of fuselage bay panels, has been conducted with a total of 78 test plates (57 composite and 21 aluminium for comparison).

Pre-loading:
For this study, one tensile pre-loading level was considered: 0.25% corresponding to Design Limit Load (DLL). Two pre-loading levels were considered for the compression case: 0.5 Pb (no buckling) and 1.4 Pb/1.5 Pb (with buckling) for the composite and aluminium plates respectively. For preloading in the postbuckle region, two cases were investigated corresponding to an impact on the concave and convex face of the buckle. The reason for conducting investigation in the postbuckle region is that buckling may occur in these thin panels at DLL.

Impact damage:
Two types of damage were of interest for the composite plates: notch damage from small hard body impactors and delamination damage from blunt impactors. This means that visual impact damage (VID) of category 2 and 3 seen in routine and visual inspections are considered for the test programme. Category 4 damage (steel beam) was also addressed in the pre-screening test programme.

The Following conclusions can be drawn from the experimental results:

- For the aluminium plates there was no significant interaction between tension/compression preload and impact damage, at the DLL preload levels considered, which caused reduction in residual strengths.
- For the composite plates in tension there were small reductions in residual strengths for both blunt and notch impacts. They were not very significant for the low preloads at DLL level studied here.
- For the composite plates in compression with notch damage, which were all tested and failed by buckling, there was no significant reduction in residual compression strengths. At buckling failure the high failure strains were away from the central damage and holes (due to the observed buckling mode), which may explain the small influence of pre-loading on the residual strength. If the buckling mode were different, results may have been different
- The composite plates in compression with blunt impact causing delamination damage were the most critical cases studied. Delaminations grew with quasi-static loads which had a strong influence on bending strengths and hence reduced buckling failure loads.

This first study shows that compression pre-load and blunt impact may be a critical case for composite panels. This was especially seen in the DLR study for a specific plate configuration (lay-up, dimensions), and specific load cases (0.5 Pb → before buckling, 1.4 Pb → after buckling).

8 Recommendations

The DLR test programme was based on test specimens at Level 1 and Level 2 of the test pyramid, with a range of load cases and impact scenarios chosen to be relevant to aircraft panel structures. The results are not conclusive, but were consistent with previous studies in the literature which used smaller, idealised test specimens and more severe load conditions. With this premise, the recommendations from the LIBCOS study for EASA to consider are:

1. For composite panel structures subjected to tensile preloads DT certification requirements based on impact tests on stress-free structures, with residual strength tests on damaged specimens, are sufficient for structural safety without extending impact test requirements to prestressed structures. This is the case because current DLL values are low for composites in tension, with high safety margins at DUL.
2. For composite panel structures subjected to compression preloads the findings are less conclusive. For high energy hard body impact (VID, Cat 3) with localised notch damage and penetration there was no significant reduction in panel residual strengths with compression preload, thus current requirements appear to be adequate. For low energy blunt impacts (BVID, Cat 1, Cat 2) the extent of delamination damage was sensitive to the local stress state at the impact position, which caused greater reductions in residual strength and could cause a smaller or zero safety margin at DUL. Pending further fundamental studies (such as 3 and 4 below), Damage Tolerance guidance material could be developed to require that preload be accounted for when defining damage i.e. Categories per AMC 20-29, in relation to its detection and residual strength.
3. DLR recommends additional tests on composite panels at Level 1 or 2 with compression and/or shear preload for blunt impact causing BVID damage, with plate geometries chosen to provide a range of local stress states at impact, from pure compression or shear (thicker or constrained specimens), alternative buckling modes (variation in panel geometry) and with increased damage area through higher energy impacts.
4. It is also recommended to extend the programme to realistic composite panels by tests with compression preload on Level 3 composite structures, such as stringer stiffened panels, impacted both on the preloaded stringer and between stringers.
5. For aluminium panel structures subjected to tensile and compression preloads there was no significant change in residual strength with notch impact damage, thus current DT certification procedures with impact tests on stress-free structures do not require modification .

9 References

1. Hachenberg, D., The role of Advanced Numerical Methods in the Design and Certification of Future Composite Aircraft Structures, WCCM V, Vienna, July 2002.
2. FAR Part 25 -Airworthiness standards: Transport Category Airplane, Special Federal Aviation Regulations.
3. JAA EASA Certification Specifications for Large Aircraft, EASA CS-25 superseded by EASA AMC 20-29.
4. ACJ 25.603: Acceptable Means of Compliance to FAR 25 for composite materials
5. EASA AMC 20-29, Annex II, 26/07/2010
6. FAA Advisory Circular AC 20.107A Composite Aircraft Structures
7. CMH-17, Composite Materials Handbook, www.cmh17.org
8. Irving, P.E. et al, Effect of preload on bird strike damage in carbon fibre polymer composite beams, CAA Report, Cranfield University, CU/WA9/W30814E/62, 2004.
9. Zhang, Z., Davies, G.A.O., Hitchings, D., Impact damage with compressive preload and post-impact compression of carbon composite plates. *Int J Impact Eng*, vol. 22, 485-509, 1999.
10. Heimbs, S., Heller, S., Middendorf, P., Hähnel, H., Weiße, J., Low velocity impact on CFRP plates with compressive preload: Test and modelling, *Int. J. of Impact Engineering*, *Vol 36, 10-11*, *1182-1193, 2009.*
11. Whittingham, B., Marshall, I.H., Mitrevski, T., Jones, R., The response of composite structures with pre-stress subject to low velocity impact damage. *Compos Struct*, vol.66, 685-698, 2004.
12. Pickett, A.K. Fouinneteau, M.R.C., Middendorf, P. Test and modelling of impact on pre-loaded composite panels, Appl. Comp. Mats, 16, Sept. 2009.
13. AIA Project Report on High Bypass Ratio Turbine Engine Uncontained Rotor Events and Small Fragment Threat Characterisation 1969-2006, Volume 1, 1969-2006 High Bypass Commercial Turbofans, January 2010
14. FAA AC No. 20-128A, Design considerations for minimizing hazards caused by uncontained turbine engine and auxíliary power unit rotor failure, US Department of transportations, Federal Aviation Administration, 3/25/1997
15. C:E: Frankenberger, III, Small-Engine Uncontained Debris Analysis, DOT/FAA/AR-99/7, Final report, US Department of Transportations, Federal Aviation Adminisatration, Feb. 1999
16. CMH-17 (in development), Atlanta proceedings, 4.19.2010
17. Wu, D.; Salerno, A.; Malter, U.; Aoki, R.; Kochendörfer, R.; Kächele, P.K.; Woithe, K.; Pfister, K.; Busse, G.; Inspection of aircraft structural components using lockin-thermography; Quantitative infrared thermography, QIRT 96, Eurotherm Series 50, Balageas, D.; Busse, G.; Carlomagno, G.M.; (Eds), pp 251-256, 1997
18. CELPACT: Cellular Structures for Impact Performance, FP6-2005-Aero-1-0310382, 2006 – 2009.
19. ALCAS: Advanced Low-cost Aircraft Structures IP, FP6-2003-Aero-1, 2005 - 2010.
20. Kaletta, P., Advanced numerical optimisation of laminate stacking sequence using a load categorisation approach, ECCM 2010, IV European Conf. on Computational Mechanics, Paris, May 16-21 2010.

21. Sierakowski, R.L., Newaz, G.M., *Damage tolerance in advanced composites*, Technomic, Lancaster PA, 1995.

22. Abrate, S. *Impact on composite structures*, Cambridge University Press, 1998.

23. Dorey, G., Fracture behaviour and residual strength of carbon fibre composites subjected to impact loads, AGARD-CP-163, Munich, October 1974.

24. Soutis, C., Curtis, P.T., Prediction of post-impact compressive strength of CFRP laminated composites, Comp. Sci. Tech. **56**, 677-684, 1996.

25. Hosur, M.V., Murthy, C.R.L., Ramurthy, T.S., Compression after impact testing of carbon fiber reinforced plastic laminates, J. Comp. Technology & Research, **21**/2, 51-64, ASTM, 1999.

26. Sankar, B.V.; Sun, C.T., Low-velocity impact damage in graphite-epoxy laminates subjected to tensile initial stresses. AIAA Journal, 24/3, 1986, pp. 470-471.

27. Avva, V.S.; Vala, J.R.; Jeyaseelan, M., Effect of impact and fatigue loads on the strength of graphite/epoxy composites. In: J. M. Whitney (ed) Composite materials: testing and design (7th Conference), ASTM STP 893, 1986, 196-206.

28. Herszberg, I.; Weller, T.; Leong, K.H.; Bannister, M.K.: The residual tensile strength of stitched and unstitched carbon/epoxy laminates impacted under tensile load. In: Proceedings of the first Australasian congress on applied mechanics, Melbourne, Australia, 1996, pp. 309-314

29. Garcia-Castillo, S.K.; Sanchez-Saez, S.; Lopez-Puente, J.; Barbero, E.; Navarro, C.: Impact behaviour of preloaded glass/polyester woven plates. Composites Science and Technology, Vol. 69, 2009, pp. 711-717

30. Wiedenmann, N., Dharan, C.K.H., Ballistic penetration of compressively loads composite plates, J Comp. Materials, 40/12, 1041 – 1061,2006.

31. Starnes, J.H.; Rhodes, M.D.; Williams, J.G.: Effect of impact damage and holes on the compressive strength of a graphite/epoxy laminate. In: R. B. Pipes (ed.) Nondestructive evaluation and flaw criticality for composite materials, ASTM STP 696, 1979, pp. 145-171

32. Morlo, H.; Kunz, J.: Impact behaviour of loaded composites. 4th European Conference on Composite Materials, September 25-28, Stuttgart, 1990.

33. Nettles, A.T.; Lance, D.G.: The effects of compressive preloads on the compression-after-impact strength of carbon/epoxy. NASA Technical Paper 3303, 1992

Annex A: Summary tables of LIBCOS test results

Table A1: Pre-screening tests: Composite plates with tension preload

Plate number	Impact case	Preload % strain	Impact Mass 10^{-3} kg	Velocity m/s	Impact energy J	Q/S test failure load kN	Residual strength factor	Comments
Baseline strength test on undamaged plate								
CP001	No impact					221.8 Failed in tabs		200 mm wide plate specimen. Failed in tabs at 0.81 % strain, well below predicted failue load. Re-design tabs/bond for tension tests.
CP007	No impact					a) 217.8 1.54% strain b) 195.6 1.45% strain	1	2 x 100 mm wide Q/S test to failure a) with ductile adhesive b) with GRP tabs **Baseline 200 mm strength: 435.6 kN**
Notch impact damage								
CP002	Steel beam 109x30x4 mm	0.25%	100.8	67.0	242.4	208.8	0.48	Notch damage + large delamination
CP003	Steel beam 109x30x4 mm	0.05%	101.0	71.0	254.6	160.3	0.37	Notch damage + large delamination
CP005	12 mm steel cube	0.25%	13.0	103.7	69.9	215.05	0.49	Cube penetrated plate, square hole
CP006	12 mm steel cube	0.25%	13.3	63.9	27.2	233	0.53	Cube rebounded Square flap damage, with delamination
Delamination damage								
CP004	Rubber beam 133x31x25 mm	0.25%	101.2	99.2	497	No Q/S test	1	No damage seen in C-scan or thermography
CP008	24 mm glass ball	0.25%	18	63.8	36.6	328.6	0.75	No damage front, delam damage back
CP009	24 mm glass ball	0.25%	18	67.6	41.1	287.1	0.66	Dent at front, delam damage back

Table A2: Pre-screening tests: Composite plates with compression preload

Plate number	Impact case	Preload % strain	Impact Mass 10^{-3} kg	Velocity m/s	Impact energy J	Q/S test failure load kN	Residual strength factor	Comments
Baseline strength test on undamaged plate								
CP010	No impact	C				Buckle load: 38 kN Ult load: 132.4 kN max. displ. 4.6 mm	1	Baseline buckling load and compression strength 3-cell buckle **Pb = 38 kN**
Notch impact damage								
CP011	12 mm steel cube	**1.4 Pb** 52 kN 0.17 % strain	13.4	135.9	127.2	Ult load: 135.6 kN max. displ: 4.5 mm	1.02	Cube passed through plate, square hole , delam damage at back face Large buckle, impact on **convex** face **Q/S test:** buckle towards impact face
CP012	12 mm steel cube	**0.95 Pb** 36kN 0.12% strain	13.4	135	122.0	Ult load: 127.2 kN max. displ: 4.2 mm	0.96	Cube passed through plate, square hole , delam damage at back face Large buckle, impact on **convex** face **Q/S test:** buckle towards impact face
CP013	12 mm steel cube	5 bar 2 kN 0.05% strain	13.4	134	120.4	Ult load: 132.8 kN max. displ: 4.8 mm	1.00	Cube passed through plate, square hole , delam damage at back face No buckle in HVI test. **Q/S test:** buckle towards back face
Delamination damage								
CP014	25 mm glass ball	5 bar 2 kN 0.02%	20.2	85.6	74	Ult load: 111.7 kN max. displ: 3.5 mm	0.84	Glass ball rebounded – dent on front face and delamination on back face **Q/S test:** buckle towards back face
CP015	25 mm glass ball	**0.95 Pb** 40 bar 36 kN 0.12 %	20.2	83.3	70.1	Ult load: 88.4 kN max. displ: 2.6 mm	0.67	Glass ball rebounded - dent on front face and delamination on back face. NO FILM !!! Large buckle, impact on **convex** face **Q/S test:** buckle towards back face

Table A3: Pre-screening tests: Aluminium plates with tension or compression preload

Plate number	Impact case	Preload % strain	Impact Mass 10^{-3} kg	Velocity m/s	Impact energy J	Q/S test failure load kN	Residual strength factor	Comments
Baseline strength test on undamaged plate								
AP001	No impact	T				Yield: 158 kN Ult load: 182.5 kN max. displ. 34 mm	1	Baseline tensile strength of undamaged plate **Baseline strength: 182.5 kN**
AP003	No impact	C				Buckle load: 20 kN max load: 58.6 kN max. displ. 5 mm	1	Baseline buckling load and compression strength, 3-cell buckle, **Pb = 20 kN** After buckling plastic flow set in at constant max. load test stopped at 5 mm displ. No ultimate fracture.
Notch and indentation impact damage								
AP002	Steel beam 109x30x4 mm	T 0.23%	100.3	100.7	509	138.4	0.76	Beam passed through plate, rectangular notch ~ 30 mm long **Q/S test:** cracks extended from notch under tensile loads, causing brittle fracture
AP004	12 mm steel cube	**1.5 Pb** C 30 KN 0.15%	13.4	133.9	120.1	53 kN max. displ. 2.1 mm	0.93	Large buckle, impact on **convex** face Cube passed through plate, square hole with plastic deformation **Q/S test: Plate buckled prematurely at support edge, ca 53 kN, dropped to 30 kN**

Table A4: Main tests: Composite plates with tension preload:

Plate number	Impact case	Preload % strain	Impact Mass 10^{-3} kg	Velocity m/s	Impact energy J	Q/S test failure load kN	Residual strength factor	Comments
Baseline strength test on undamaged plate								
CP007a (P)	No impact					217.8 1.54% strain		100 mm wide Q/S test to failure with new adhesive **Baseline 200 mm strength P: 435.6 kN**
C022 (B)	No impact					431.6 1.50 % strain		**Baseline strength B: 431.6 kN**
C042 (C)	No impact					419.9 1.50 % strain		**Baseline strength C: 419.9 kN**
C048 (D)	No impact					409.4 displ. 12.3 mm		**Baseline strength D: 409.4 kN**
Notch impact damage								
C025 (B)	12 mm steel cube	0.02%	13.4	100.6	67.8	215.7 displ. 5.7 mm	0.50	Square hole notch damage + delamination
C027 (B)	12 mm steel cube	0.02%	13.4	98.5	65.0	248.7 displ. 6.6 mm	0.58	Square hole notch damage + delamination
C043 (C)	12 mm steel cube	0.02%	13.4	84.5	47.9	250.1 displ. 6.6 mm	0.60	Low velocity, old sabot left in sabot catcher Rebound with notch damage + delamination
C028 (B)	12 mm steel cube	0.02%	13.4	97.5	63.6	259.5 displ. 7.25 mm	0.60	Repeat C043, square hole notch damage + delamination
C029 (B)	12 mm steel cube	0.02%	13.4	96.7	62.7	220.3 displ. 6.0 mm	0.51	Flat impact with square hole notch damage and delamination. Q/S: Linear to failure
C030 (B)	12 mm steel cube	0.15%	13.4	93.4	58.4	206.5 displ. 5.6 mm	0.48	Corner impact with notch damage and delamination Q/S Diamond notch

CP005 (P)	12 mm steel cube	0.25%	13	103.7	69.9	215.05 displ. 6.0 mm	0.49	Cube penetrated plate, square hole
C026 (B)	12 mm steel cube	0.25%	13.4	103.1	71.2	211.1 displ. 5.6 mm	0.49	Square hole notch damage + delamination
C041 (C)	12 mm steel cube	0.25%	13.4	101.8	69.5	256.6 displ. 7.1 mm	0.61	Square hole notch damage + delamination
C044 (C)	12 mm steel cube	0.25%	13.4	97.8	64.1	211.8 displ. 5.7 mm	0.50	Square hole notch damage + delamination
Delamination impact damage								
C023 (B)	25.2 mm glass ball	0.02%	21.0	69.7	51	291.0 displ. 7.9 mm	0.67	Rebound with small mark at front, delam at back
C045 (D)	25.2 mm glass ball	0.02%	21.3	64.9	44.8	311.1 displ. 8.7 mm	0.76	Rebound with delamination at back
C046 (D)	25.2 mm glass ball	0.02%	21.3	65.2	45.3	301.0 displ. 8.5 mm	0.74	Rebound with delamination at back
C032 (B)	25.2 mm glass ball	0.02%	21.2	63.9	43.3	326.9 displ. 9.2 mm	0.76	Rebound with small delamination at back face.
C031 (B)	25.2 mm glass ball	0.15%	21.0	68.1	48.7	225.2 displ. 6.1 mm	0.52	0.15% prestrain: Rebound with delamination damage at back face
CP008 (P)	24 mm glass ball	0.25%	18	63.8	36.6	328.6 displ. 9.9 mm	0.75	No damage front, delam damage back
CP009 (B)	24 mm glass ball	0.25%	18	67.6	41.1	287.1 displ. 8.0 mm	0.66	Dent at front, delam damage back
C024 (B)	25.2 mm glass ball	0.25%	20.9	67.6	47.7	273.1 displ. 7.9 mm	0.63	Rebound with small mark at front, delam at back. NO FILM
C047 (D)	25.2 mm glass ball	0.25%	21.3	64.4	44.2	266.4 displ. 7.6 mm	0.65	Rebound with delamination at back

Table A5: Main tests: Composite plates with compression preload

Plate number	Impact case	Preload % strain	Impact Mass 10^{-3} kg	Velocity m/s	Impact energy J	Q/S test failure load kN	Residual strength factor	Comments
Baseline strength test on undamaged plate								
CP010 (A)	No impact	C				Buckle load: 38 kN Ult load: 132.4 kN max. displ: 4.6 mm	**1** **(A: 132.4 kN)**	Baseline buckling load and compression strength 3-cell buckle **Pb = 38 kN** **Specimen cut from Plate A**
C035 (F)	No impact	C				Buckle load: 38 kN Ult load: 119.1 kN max. displ: 4.0 mm	**1** **(F: 119.1 kN**	Baseline buckling load and compression strength 3-cell buckle **Pb ~ 38 kN** **Specimen cut from Plate F**
C036 (F)	No impact	C				Buckle load: 38 kN Ult load: 118.5 kN max. displ: 4.0 mm	**1** **(F: 118.8 kN**	Baseline buckling load and compression strength 3-cell buckle **Pb ~ 38 kN** **Specimen cut from Plate F**
C060 (H)	No impact	C				Buckle load: 38 kN Ult load: 133.2 kN max. displ: 4.5 mm	**1** **(H: 133.2 kN**	Baseline buckling load and compression strength 3-cell buckle **Pb ~ 38 kN** **Specimen cut from reserve plate H**
Notch impact damage								
CP013 (A)	12 mm steel cube	5 bar 2 kN 0.05% strain	13.4	134	120.4	Ult load: 132.8 kN max. displ: 4.8 mm	1.00	Cube passed through plate, square hole , delam damage at back face No buckle in HVI test. **Q/S test:** buckle towards back face
C018 (A)	12 mm steel cube	10 bar 5 kN	13.4	131.6	116	Ult load: 126.8 kN max. displ: 4.2 mm	0.96	Cube passed through plate, square hole , delam damage at back face No buckle in HVI test. **Q/S test:** buckle towards back face
C019 (A)	12 mm steel cube	5 bar 2 kN	13.4	135.0	122	Ult load: 127.0 kN max. displ: 4.4 mm	0.96	Cube passed through plate, square hole , delam damage at back face

								No buckle in HVI test. **Q/S test:** buckle towards back face
C053 (H)	12 mm steel cube	**0.5 Pb** 25 bar 20 kN 0.75 0/00	13.4	136.4	124.7	Ult load: 129.6 kN max. displ: 4.4 mm	0.97	Preload 25 bar, calibrated force 20 kN., ave. DMS 0.75 0/00. Light convex buckle (ca 1 mm). Corner impact with notch damage. **Q/S test:** buckle towards impact face
C054 (H)	12 mm steel cube	**0.5 Pb** 25 bar 20 kN 0.75 0/00	13.4	129.2	111.8	Ult load: 124.1 kN max. displ: 4.2 mm	0.93	Flat impact, diamond shaped notch. Light convex buckle (ca 1 mm). **Q/S test:** buckle towards impact face
C055 (H)	12 mm steel cube	**0.5 Pb** 25 bar 20 kN 0.7 0/00	13.4	128.2	110.1	Ult load: 135.9 kN max. displ: 4.6 mm	1.02	Flat impact square notch. Light convex buckle (1 mm) **Q/S test:** buckle towards back face
CP011 (A)	12 mm steel cube	**1.4 Pb** 52 kN 0.17 % strain	13.4	135.9	127.2	Ult load: 135.6 kN max. displ: 4.5 mm	1.02	Cube passed through plate, square hole , delam damage at back face Large buckle, impact on **convex** face **Preload is 1.38 Pb – after cylinder calibration** **Q/S test:** buckle towards impact face
C016 (A)	12 mm steel cube	**1.4 Pb** 55 bar 53.2 kN	13.4	129.2	111.8	Ult load: 119.0 kN (124.9 kN before corr.) max. displ: 3.2 mm	0.90	Cube passed through plate, square hole , delam damage at back face Large buckle, impact on **convex** face **Preload is 1.4 Pb** **Q/S test:** buckle towards rear face Curve corrected as loaded on bolt which failed
C020 (A)	12 mm steel cube	**1.4 Pb** 55 bar 53.2 kN	13.4	126.6	107.4	Ult load: 117.6 kN max. displ: 3.7 mm	0.89	Cube passed through plate, square hole , delam damage at back face Large buckle, impact on **convex** face **Preload is 1.4 Pb** **Q/S test:** buckle towards impact face
C021 (A)	12 mm steel cube	**1.4 Pb** 55 bar 53.2 kN	13.4	93.5	58.5	Ult load: 124.9 kN max. displ: 3.2 mm	0.94	Cube stopped by plate bounced back, front face damage , delam damage at back face. Reduced impact velocity due to sabot in gun.

								Large buckle, impact on **concave** face **Preload is 1.4 Pb** **Q/S test:** buckle towards impact face
Delamination damage								
CP014 (A)	25 mm glass ball	5 bar 2 kN 0.02%	20.2	85.6	74	Ult load: 111.7 kN max. displ: 3.5 mm	0.84	Glass ball rebounded – dent on front face and delamination on back face **Q/S test:** buckle towards back face
C037 (F)	25 mm glass ball	5 bar 2 kN 0.01%	20.4	81.8	64.5	Ult load: 100.5 kN max. displ: 3.6 mm	0.85	Glass ball rebounded – dent on front face and delamination on back face **Q/S test:** buckle to back face, some bending at top edge
C059 (H)	25.2 mm glass ball	5 bar 2 kN 0.1 0/00	21.0	77.6	63.3	Ult load: 122.8 kN max. displ: 4.3 mm	0.92	Glass ball rebounded – dent on front face and delamination on back face Light buckle (1 mm), impact on convex face
C056 (H)	25.2 mm glass ball	**0.5 Pb** 25 bar 20 kN 0.7 0/00	21.0	79.7	66.8	Ult load: 93.9 kN max. displ: 3.0 mm	0.70	Glass ball rebounded – dent on front face and delamination on back face Light buckle (1 mm), impact on **convex** face
C057 (H)	25.2 mm glass ball	**0.5 Pb** 25 bar 20 kN 0.7 0/00	21.0	80.0	67.2	Ult load: 87.9 kN max. displ: 2.6 mm	0.66	Glass ball rebounded – dent on front face and delamination on back face Light buckle (1 mm), impact on convex face NO FILM. Estimated velocity. Off-centre impact (~2cm)
C058 (H)	25.2 mm glass ball	**0.5 Pb** 25 bar 20 kN 0.7 0/00	21.0	76.8	61.9	Ult load: 89.6kN max. displ: 2.8 mm	0.67	Glass ball rebounded – dent on front face and delamination on back face Light buckle (1 mm), impact on convex face
C017 (A)	24.5 mm glass ball	**1.4 Pb** 55 bar 53.2 kN	19.3	82.2	65.2	Ult load: 85.1 kN max. displ: 2.6 mm	0.64	Glass ball rebounded – dent on front face and delamination on back face Large buckle, impact on **convex** face **Q/S test:** 2 buckles in plate (S shape) Fractured in middle
C034 (F)	24.5 mm glass ball	**1.4 Pb** 55 bar	19.3	83.4	67.1	Ult load: 58.7 kN max. displ: 3.2 mm	0.49	Glass ball rebounded – dent on front face and

		53.2 kN						delamination on back face Large buckle, impact on **convex** face **Q/S test:** buckle to back face, some bending at top edge
C039 (F)	24.1 mm glass ball	**1.4 Pb** 55 bar 53.2 kN	18.0	80.6	58.4	Ult load: 80.7 kN max. displ: 2.8 mm	0.68	Glass ball rebounded – dent on front face and delamination on back face Large buckle, impact on **convex** face **Q/S test:** buckle to back face
C033 (F)	24.5 mm glass ball	**1.4 Pb** 55 bar 53.2 kN	19.3	85.7	70.9	Ult load: 87.7 kN max. displ: 3.4 mm	0.74	Glass ball rebounded – dent on front face and delamination on back face Large buckle, impact on **concave** face with more visible damage than C034 **Q/S test:** buckle to back face
C038 (F)	24.5 mm glass ball	**1.4 Pb** 55 bar 53.2 kN	18.9	78.8	58.7	Ult load: 96.9 kN max. displ: 3.9 mm	0.82	Glass ball rebounded – dent on front face and delamination on back face Large buckle, impact on **concave** face **Q/S test:** buckle to back face. Local buckle first (at top?) at 90 kN, 3.2 mm
C040 (F)	23.9 mm glass ball	**1.4 Pb** 55 bar 53.2 kN	17.9	82.4	60.8	Ult load: 87.0 kN max. displ: 2.6 mm	0.73	Glass ball rebounded – dent on front face and delamination on back face Large buckle, impact on **concave** face Extended supports **Q/S test:** buckle to back face, fracture in middle

Table A6: Main tests: Aluminium plates with tension preload

Plate number	Impact case	Preload % strain	Impact Mass 10^{-3} kg	Velocity m/s	Impact energy J	Q/S test failure load kN	Residual strength factor	Comments
Baseline strength test on undamaged plate								
AP001	No impact	T				Yield: 158 kN Ult load: 182.5 kN Max. displ. 34 mm		Baseline tensile strength of undamaged plate
A013	No impact	T				170 kN 21.2 mm		Baseline tensile strength of undamaged plate **Mean value: 176.3 kN**
Notch and indentation impact damage								
A014	12 mm steel cube	0.02%	13.4	133.7	119.7	144.4 displ. 4.6 mm	0.82	**Rebound** + indentation with small edge crack (23 mm)
A015	12 mm steel cube	0.02%	13.4	142.7	136.3	163.0 displ. 10.8 mm	0.92	**Rebound** + indentation with no crack. Large pl. deformation in Q/S test, with no fracture. Test stopped at 10.8 mm displ. Tabs adhesive failed.
A020	12 mm steel cube	0.02%	13.4	147.9	146.6	143.2 displ. 4.5 mm	0.81	Flat impact, with **rebound** causing indent plus 3 cracks, 12 mm in size. Q/S. 2 cracks developed at notch
A017	12 mm steel cube	0.02%	13.4	171.5	197.1	148.4 displ. 4.4 mm	0.84	**Notch** damage, square hole (15 mm)
A021	12 mm steel cube	0.25%	13.4	92.9	57.9	145.8 displ. 4.5 mm	0.83	Lower velocity intended to cause indent. Impact was at corner point, led to **rebound** with indent, but with 20 mm wide crack in plate. Q/S. 2 cracks developed at notch
A016	12 mm steel cube	0.25%	13.4	145.1	141.1	123.7 displ. 3.9 mm	0.70	**Notch** damage, square hole (35 mm)

A018	12 mm steel cube	0.25%	13.4	141.6	134.4	151.7 displ. 5.2 mm	0.86	**Notch** damage, square hole (23 mm). NO HVI FILM
A019	12 mm steel cube	0.25%	13.4	141.2	133.6	143.8 displ. 4.5 mm	0.82	**Notch** damage, rectangular hole 22 mm wide by 25 mm long, with 20 mm high flap. Q/S. 2 cracks developed at notch

Table A7: Main tests: Aluminium plates with compression preload

Plate number	Impact case	Preload % strain	Impact Mass 10^{-3} kg	Velocity m/s	Impact energy J	Q/S test failure load kN	Residual strength factor	Comments
Baseline strength test on undamaged plate								
AP003	No impact					Buckle load: 20 kN Max load: 58.6 kN	1	Baseline buckling load and compression strength, 3-cell buckle, **Pb = 20 kN** After buckling plastic flow set in at constant max. load test stopped at 5 mm displ. No ultimate fracture.
A007	No impact					Buckle load: 20 kN Max load: 55.5 kN	1	Baseline buckling load and compression strength, 3-cell buckle, **Pb = 20 kN** After buckling plastic flow set in at constant max. load, test stopped at 5 mm displ. No ultimate fracture. **Mean comp. str 57.1 kN**
Notch and indentation impact damage								
A012	12 mm steel cube	5 bar C 2 kN	13.4	89.6	53.8	55.7 kN 5 mm	0.98	Cube stopped by plate with **rebound**, indentation with very small crack from cube corner. **Preload is 1.5 Pb** **Q/S test:** buckle to back face, rail bolt deformed
A008	12 mm steel cube	5 bar C 2 kN	13.5	123.2	102.4	56.9 kN 5 mm	0.996	Cube **stopped** by plate, drops to front, crack with plastic deformation **Q/S test:** extended rails, buckle to back face, top edge buckle at 40 kN, 1.4 mm
A006	12 mm steel cube	5 bar C 2 KN	13.4	121.7	99.2	54.3 kN 5 mm	0.95	Cube passed through plate, large square hole with plastic deformation **Q/S test:** 3 cell buckle, stopped at 5 mm
A009	12 mm steel cube	5 bar C 2 kN	13.4	131.4	115.7	57.9 kN 5 mm	1.01	Cube passed through plate, large square hole with plastic deformation **Q/S test:** extended rails, buckle to back face, top edge buckle at 40 kN, 1.4 mm
A010	12 mm steel cube	**1.5 Pb** 30 bar C 30 KN	13.4	129.0	111.6	55.4 kN 5 mm	0.97	Large buckle, impact on **convex** face Cube stopped by plate with **rebound**, square indentation in buckle, no crack. **Preload is 1.5 Pb**

								Q/S test: extended rails, buckle to back face, kink at 3.2 mm
A005	12 mm steel cube	**1.5 Pb** 30 bar C 30 KN 0.15%	13.4	125.6	106.5	56.9 kN 5 mm	0.996	Large buckle, impact on **convex** face Cube **stopped** in plate, square hole with plastic deformation. Central buckle plus free edge buckle at 30 kN preload **Preload is 1.5 Pb** **Q/S test:** 3 cell buckle, stopped at 5 mm
AP004	12 mm steel cube	**1.5 Pb** C 30 KN 0.15%	13.4	133.9	120.1	53 kN 2.05 mm	0.93	Large buckle, impact on **convex** face Cube passed through plate, square hole with plastic deformation **Preload is 1.5 Pb** **Q/S test: Plate buckled prematurely at support edge, ca 53 kN, dropped to 30 kN**
A011	12 mm steel cube	**1.5 Pb** 30 bar C 30 KN	13.4	129.7	112.7	56.6 kN 5 mm	0.99	Large buckle, impact on **concave** face Cube passed through plate, large square hole with plastic deformation **Preload is 1.5 Pb** **Q/S test:** buckle to back face, softer response